Badar ul Ali Zeeshan

Constructing an Innovative Base-Isolation System under Masonry Structures

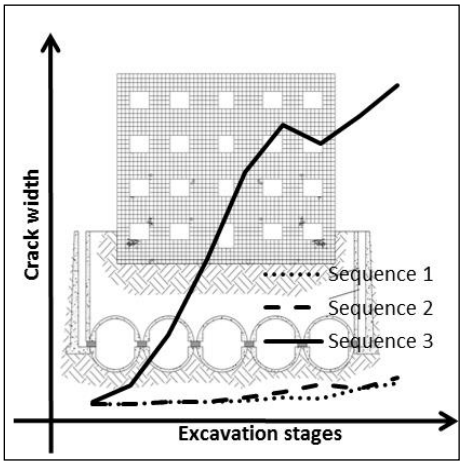

Dottorato di Ricerca in Ingegneria delle Strutture
Politecnico Di Torino

Badar ul Ali Zeeshan

Constructing an Innovative Base-Isolation System under Masonry Structures

Tesi per il conseguimento del titolo di Dottore di Ricerca
XXV Ciclo (A.A. 2010, 2011, 2012, 2013)

Dottorato di Ricerca in Ingegneria delle Strutture
Politecnico Di Torino

Dicembre 2013

Dottorato di Ricerca in Ingegneria delle Strutture
Politecnico di Torino, Corso Duca degli Abruzzi 24, 10129 Torino, Italy
Tutor: Prof. Alessandro De Stefano
Coordinator: Prof. Alberto Carpinteri

Acknowledgements

I would like to thank Prof. Alessandro De Stefano for giving me support during the research and allowing me the space and time to work with freedom. I would also like to thank Dr. Stefano Invernizzi for giving me time, support and helping me with numerical models. The work would not have been realized, had it been not for the support of my father, who inculcated, in me, the work ethics that have been central to my progress.

Abstract

Seismic up-gradation of existing buildings is a very challenging task, as it requires us to consider historical and economical aspects of building. While proposing a seismic-retrofit scheme for a historical building, one should keep in mind that it should be compatible with existing materials, be least intrusive, monitorable and removable.

A novel base-isolation technique has been proposed for the up-gradation of existing buildings against seismic actions which does not involve any alteration in existing buildings, and it is monitorable and removable. The method asks for the uncoupling of soil under, and around the building, with the help of closely spaced microtunnels, trenches and retaining walls. Closely spaced microtunnels will lay under the foundation of building, running parallel to one of the dimension of the building, and base-isolation devices will be fitted in lining of these microtunnels. These closely spaced micro-tunnels, along with the trenches and retaining walls around the building, will isolate the structure from seismic actions. This assembly of microtunnels, fitted with isolation devices, and trenches, around the building, will be able to filter seismic forces in both directions of building.

The construction of these micro-tunnels, for realisation of innovative base-isolation technique, is the most critical phase, because it can have a detrimental effect on building. This work explores the potential applicability of the novel base-isolation method on masonry buildings by assessing susceptibility of masonry wall, having different physical and material characteristics, to damage (relating to aesthetic of building) inflicted by the construction of microtunnels in various soil conditions. The effect of transverse ground movements is considered in this study. A parametric study is conducted using 2-D (coupled) nonlinear finite element analyses, considering factors such as strength and stiffness of masonry, stiffness of soil, soil-structure interface, excavation sequence of tunnels, different physical characteristics of wall and depth of tunnels.

The study shows the applicability of innovative base-isolation technique, highlights the vulnerability levels of walls of different physical characteristics, emphasizes the importance of excavation sequence of microtunnels in reducing risk of damage, and mentions symptoms that correlate with damage.

Index

Chapter 1

Introduction

1.1. Background

Seismic upgrading of buildings has always been a challenging task for structural engineers. More so, if the building, in question, is a part of cultural heritage of a society. Societies preserve buildings of historic importance from natural hazards as these buildings are part of their identity; cultural heritage educate people about older generations and can remind them about certain event of historical significance.

The technique adopted for up-gradation of historical building must employ compatible and durable materials, should be based on principle of minimum intervention, and must preserve the architectural elements that define the building. The strengthening measures, used in the method, must be monitorable and removable.

Many retrofitting methods have been devised in past years which may result in addition or removal of structural elements in existing building, structural repointing, injection of grout, and jacketing among others. These techniques are intrusive in nature and are not always applicable as they may not preserve the architectural features of building. Base isolation has also been used to

strengthen historical buildings against seismic loads. Base isolation is the least intrusive technique, but it is not removal and reversible.

An innovative method of isolating structure from the adverse effects of ground excitation has been proposed by Clemente et al. [1]. The method uncouples the soil under, and around, the building from the surrounding soil with the help of closely spaced microtunnels, trenches and retaining walls. Microtunnels will be excavated under the foundation of building, covering entire dimension in transverse direction, and dampers will be fitted within the linings of these microtunnels. These closely spaced micro-tunnels, along with the trenches and retaining walls around the building, will isolate the structure from seismic actions. This system has been given diagrammatic presentation in Figure 1.1.

The construction of microtunnels is very critical phase of installing this innovative base isolation system as excavation process will result in subsidence of ground which can damage the existing building. Hence it is very important to estimate the damage inflicted by construction of closely spaced microtunnels on walls of different physical and mechanical characteristics in variety of soil conditions, which will help us in showing applicability, as well as limitations, of this innovative base-isolation technique.

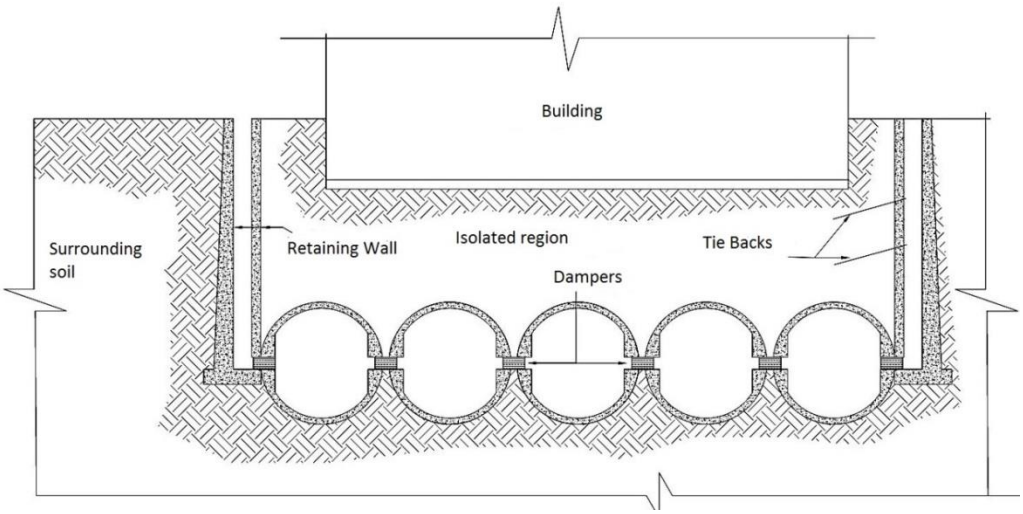

Figure 1.1: Schematization of innovative base-isolation technique

1.2. Objectives/Scope of research

Objective of this research work is to evaluate the suitability of employing the base isolation technique, proposed by Clemente et al. [1], on historic masonry buildings by assessing the damage susceptibility of masonry walls, of different geometric and mechanical characteristics, to the transverse ground movements, induced by construction of closely-spaced microtunnels (required for innovative base isolation technique), in different soil conditions.

Different geometric configurations of masonry wall are selected to investigate the effect opening configurations, length and height of wall on damage-susceptibility; each type of wall is subjected to sequential microtunneling operations in soil of different mechanical properties, considering soil-structure interaction. The effect of sequence of excavation is also considered by investigating different sequences for each case. Different mechanical properties, representing range of conditions of historic construction, for masonry are chosen for a wall of particular geometric configuration. For each type of wall, soil properties and excavation sequence, which will limit the damage to aesthetics of building, is noted.

The effect of depth of tunneling, and normal stiffness of interface, on damage-susceptibility of masonry wall is also investigated.

The results will show applicability of innovative base-isolation technique. The study also encompasses behavior of different damage symptoms during excavation simulation of microtunnels. Investigation of behavior of damage symptoms can be useful for monitoring purposes.

Nonlinear, 2D and coupled finite element analysis has been performed considering factors such as geometric configuration of masonry, mechanical properties of masonry and soil, depth of tunnels, soil-structure interface, and excavation sequence of tunnels. In coupled approach, soil and masonry wall is modeled together, considering interaction between wall and soil using interface elements.

First, literature on ground movements in transverse direction, related to microtunneling operations, will be reviewed. Some of the existing literature regarding single, as well as multiple tunnels, will be presented. Methods available for damage assessment of masonry, subjected to tunneling operations, will also be discussed. The results will be presented next, indicating mechanical properties of masonry and soil corresponding to a particular level of damage for walls of different physical characteristics; results, showing behavior of wall during tunneling operation, will also be discussed; relation between damage and damage indicators will also be analyzed.

Although the problem of multiple tunneling has been addressed before, but the damage susceptibility of masonry to the sequential excavation of closely spaced microtunnels (as far as author knows) has never been addressed.

1.3. Outline of thesis

Chapter 1 introduces the reader to research work, giving background, research objectives and outline of thesis.

Chapter 2 comprises of literature review. Methods for estimating transverse Greenfield ground movements, related to tunnels, have been reviewed for single, as well as multiple tunnels. Most commonly used method for estimating vertical and horizontal ground movements in transverse direction, related to single tunnel, has been presented. Literature has also been reviewed regarding estimation of transverse greenfield ground movements for multiple tunnels. Commonly used techniques to predict the damage due to tunnel-related ground movements have also been presented.

Chapter 3 deals with methodology adopted in this study to investigate the applicability of innovative base isolation technique. The finite element model, along with adopted constitutive laws for different materials and their properties have been mentioned in this chapter. Different excavation sequences, adopted for each set of tunnels, are shown. The section also shows the methodoly to simulate sequential excavation of tunnels.

Chapter 4 presents results, as well as analysis, of this study. First four sections show results, regarding behavior of walls, requiring assembly of 6, 7, 9 and 10 tunnels. For each section, results have been divided into two categories, each corresponding to a particular type of interface. Next two sections discuss effect of depth of tunnels, and normal stiffness of interface on damage susceptibility of wall. Seventh section presents results of a study, conducted to investigate behavior of various damage indicators during simulation of closely-spaced-microtunnels.

Chapter 5 Conclusion are presented in the last section.

Chapter 2

Literature review

2.1. Vertical greenfield ground movements in soft ground in transverse direction: single tunnel

The most widely used method for estimating transverse greenfield settlements due to excavation of tunnels is the empirical method proposed by Peck (1969) [2]. This method can also be used for estimating greenfield settlements over microtunnels [3], [4].

Peck (1969) and Schmidt (1969) presented an empirical method, based on numerous field data, to estimate the vertical transverse settlement profile over single tunnel. The method uses Gaussian distribution curve. Following relation is used to compute transverse settlement profile in greenfield conditions:

$$S(x) = S_{(\max)} \cdot e^{-\frac{x^2}{2i^2}} \qquad (2.1)$$

Where $S_{(max)}$ is maximum vertical settlement above tunnel axis; '*i'* is point of inflection (trough width), measured from tunnel centerline; 'x' is settlement at the point of interest, also measured from tunnel centerline, see Figure 2.1.

2.1.1. Trough width

As defined in previous section, trough width is the distance between longitudinal axis of tunnel and point of inflection. Trough width has been related with the depth of tunnel centerline from ground surface and size of tunnel by Peck(1969) [2], Cording & Hansmire(1975) [5] and clough & Schmidt(1981) [6]. O' Reilly and New (1982) [7] analyzed the field data and found that the shape of transverse settlement profile is not related to diameter of tunnel, for depths greater than diameter of tunnel. He found following relationship for cohesive soils and non-cohesive soils:

$$i = 0.43\, Z_o + 1.1 \text{ (cohesive soils)} \quad (2.2)$$

$$i = 0.28\, Z_o - 1.1 \text{ (granular soils)} \quad (2.3)$$

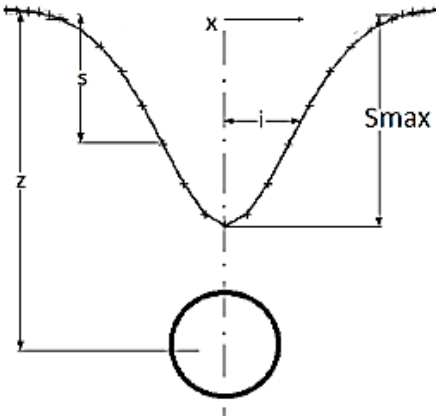

Figure 2.1: Transverse settlement profile by [2]

In the equation 2.2 and 2.3, both parameters are in meters and Z_o is depth of centerline of tunnel from ground surface. Figure 2.2 shows results of regression analysis.

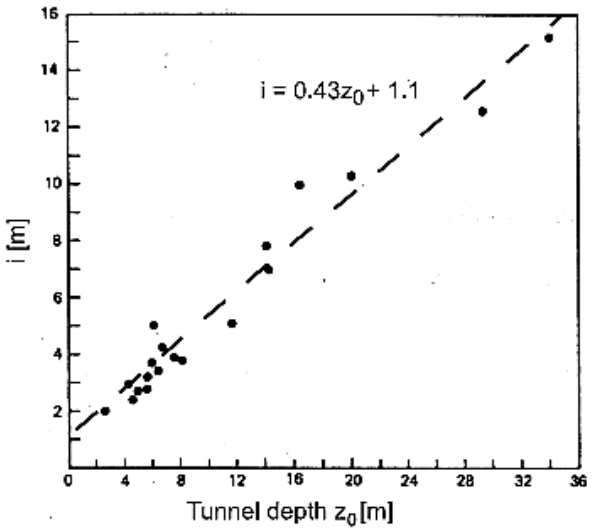

Figure 2.2: relation between point of inflection and depth of tunnel [7]

For practical purposes, O' Reilly and New (1982) [7] proposed simplified relation, as the equation 2.2 nearly passes through origin. The relation proposed is:

$$i = K \,.\, Z_o \tag{2.4}$$

In, equation 2.4, '*K*' is trough width parameter and its value for clayey soils is about 0.5, and for sandy soils is 0.25. Other authors, [8]; [9], analyzed larger set field of data and they agreed on the value of K=0.5 for clays.

2.1.2. Volume Loss

In the equation 2.1, $S_{(max)}$ has been related to the volume of settlement trough per unit length, which is the area enclosed by settlement trough, and can be computed as:

$$V_s = i \,.\, S_{max} \,.\, \sqrt{2\pi} \tag{2.5}$$

Where, V_s is volume of settlement trough per unit length.

V_s depends upon volume loss, expressed as ratio between V_s and area of tunnel per unit length. Volume loss is the difference between volume of excavation and the volume enclosed by the lining of tunnel. Volume loss depends on annular space, stability at face of tunnel, workmanship, construction procedure and alignment of tunnel.

In case of microtunneling operations, movements into the face of tunnel will be negligible, either due to face support, or due to stiffer clay, and due to size of tunnels [4]. Hence, annular space is main contributor to the volume loss. Maximum volume of settlement per unit length, in undrained conditions, can be presented as:

$$V_s = \frac{\pi}{4} . \left({D_t}^2 - {D_e}^2\right) \tag{2.6}$$

In equation 2.6, D_e is diameter of excavation and D_t is diameter of tunnel lining.

2.2. Horizontal greenfield ground movements in soft ground in transverse direction: single tunnel

Horizontal ground movements in transverse direction also inflict damage on buildings. It has been proposed that displacement vectors for horizontal ground movement in transverse direction can be assumed to be directed towards centerline of tunnel [7]. The relation for horizontal ground movements has been related to vertical ground movements as:

$$S_h(x) = \frac{x \, . \, S(x)}{Z_o} \tag{2.7}$$

In equation 2.7, $S_h(x)$ is horizontal ground displacement in transverse direction.

Theoretical maximum displacement occurs at inflection point. The horizontal strain can be computed by differentiating equation 2.7 with respect to x. Figure 2.3 shows distribution of horizontal displacements.

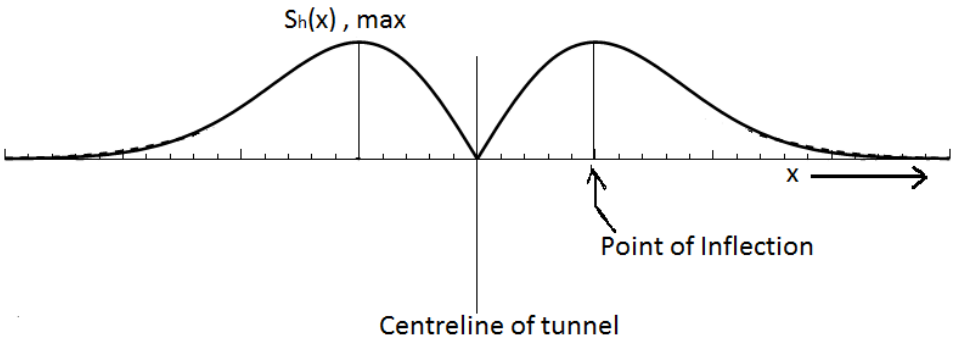

Figure 2.3: Distribution horizontal displacements at surface

2.3. Greenfield ground movements in transverse direction: multiple tunnels

Most of the work for estimating greenfield ground movements in transverse direction has been done for twin tunnels, which are required for transport infrastructure. This section reviews some of the work done for multiple tunnels.

2.3.1. Superposition method

In this method, transverse settlement trough for twin tunnels can be computed by superimposing the individual contribution of two tunnels. The method is applicable to parallel tunnels, having same depth, diameter and volume loss. This method neglects the effect of disturbance created by excavation of first tunnel and gives unacceptable results ([10]; [11]; [12]).

2.3.2. Addenbrooke and Potts 2001

Addenbrooke and Potts 2001 [10] conducted a numerical study and found the asymmetry of transverse settlement profile, associated with second tunnel, as well as noted that maximum settlement for second tunnel is more than the first one. He proposed two graphs, which can be used to modify transverse settlement profile for second tunnel.

Graphs give the modified volume loss of second tunnel, and the eccentricity of profile associated with second tunnel. Graph, Figure 2.4, shows that volume loss for second tunnel increases as the distance between tunnels decreases.

The resultant settlement profile can be obtained by adding modified settlement profile, obtained by using graphs, to the unchanged profile of first tunnel.

In the Figure 2.4, pillar width is the clear horizontal distance between tunnels.

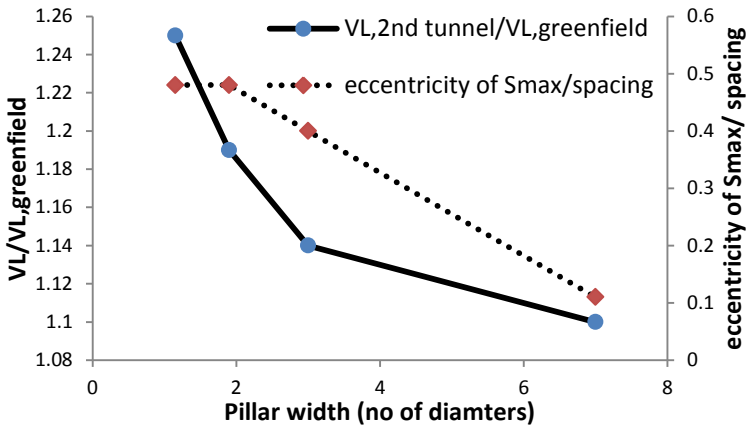

Figure 2.4: Design chart to find parameters of modified settlement trough of second tunnel, volume loss and eccentricity of maximum settlement [10]

2.3.3. Hunt 2005

Hunt performed numerical analysis and came up with a modification factor, to be applied to the empirical method [2], to estimate the transverse vertical settlement on ground surface, associated with second tunnel. The modification factor is applicable to ground movements in a region already disturbed by excavation of first tunnel. His work [13] resulted in the following relation:

$$S_{modified} = \left\{1 + \left[M\left(1 - \frac{|d+x|}{A \,.\, K^{f} \,.\, Z^{*}}\right)\right]\right\} \,.\, S \qquad (2.8)$$

In equation 2.8:

$S_{modified}$ is the modified settlement
"M" is modification factor, about 0.6 [13]
"d" is distance between axis of tunnels
"A" is multiple of '*i*' to make a half trough width (2.5-3)
" Z^*" is depth of centerline of tunnel from point of interest
" K^f" is value of K around first tunnel
" S" is settlement given by equation 2.1
Total settlement is computed by adding equations 2.1 and 2.8.

2.4. Prediction of damage due to tunneling process

Ground movements, associated with construction of tunnels, can damage adjacent buildings. Hence, the effect of tunnel-related ground movements on adjacent buildings must be assessed before carrying out an excavation process so that the appropriate excavation procedure, or preventive measures be envisaged during design phase.

Different parameters had been used in past to define deformation of building. A list of parameters (Figure 2.5), defining deformation of building, was prepared [14]. The parameters are:

- Maximum settlement experienced by building.
- Maximum differential settlement experienced by building, **ΔSmax**.
- Slope of deflection curve, **C**.
- Angular Distortion, **β.**
- Rigid body tilt, **w**.
- Angular strain, **α**.
- Deflection that defines sagging or hogging of building; measured with respect to the straight line, connecting ends of building
- Deflection ratio defined as the ratio of maximum deflection to length of building or part considered, **DR**.

This section will review empirical-analytical and numerical studies conducted over the years to predict damage associated with tunneling process.

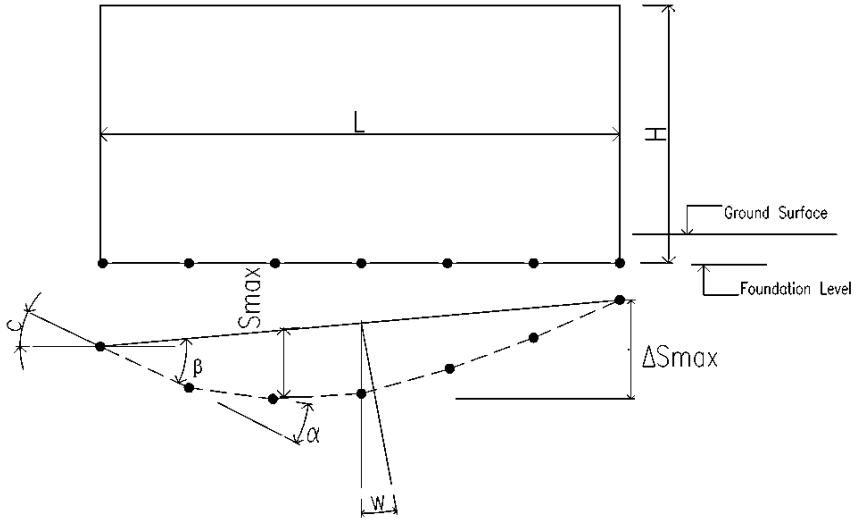

Figure 2.5: Parameters defining deformation of building [14]

2.4.1. Limiting Tensile Strength method

Limiting tensile strength method(LTSM) is empirical-analytical method and it is widely used by practicing engineers, especially during preliminary assessment of tunnel related effects on adjacent buildings. The method was proposed by Burland and Worth in 1974 and later improved by Boscardian and Cording (1989) [15].

In this method, green field settlements are imposed on wall, which is represented as isotropic, linear elastic, homogeneous and weightless beam of unit thickness; tensile strains, based on elastic beam theory [16], are calculated and a category of damage is assigned to a building. The damage category is based on concept of limiting tensile strain [17]. Limiting tensile strain is derived from critical tensile strain which is the average tensile strain in masonry on the onset of visible cracking. Critical tensile strain for masonry lies between 0.0005 to 0.00075 [14], and it was established from large scale tests on masonry. Figure 2.6 shows four stages involved in application of LTSM.

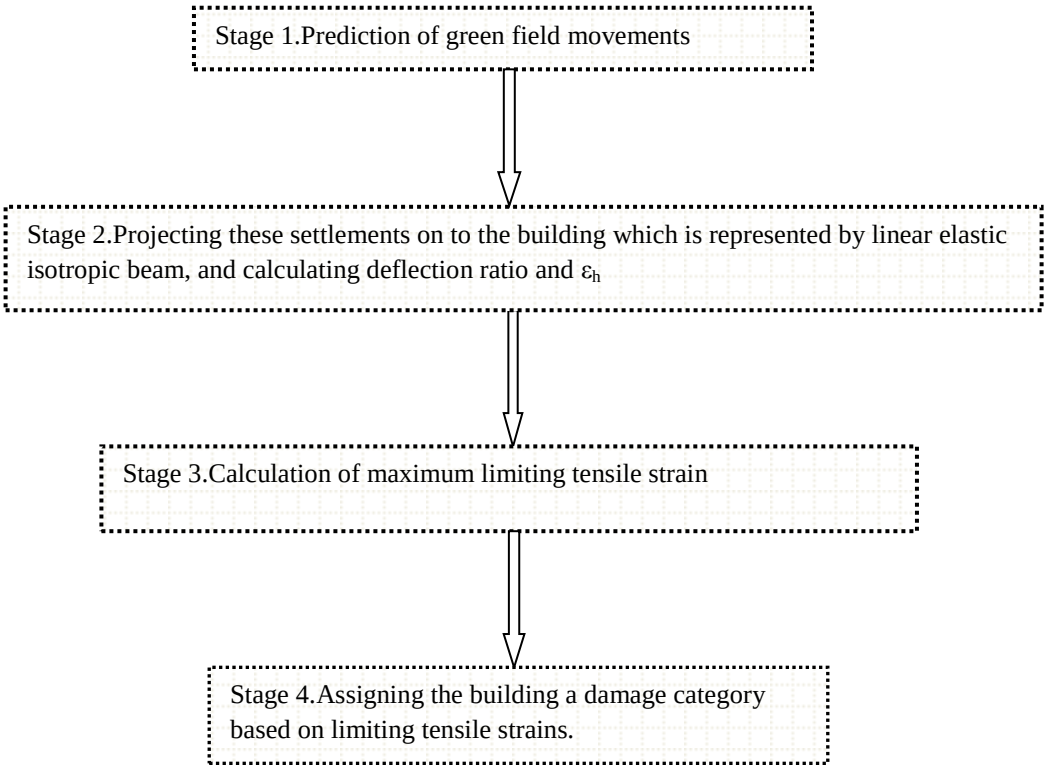

Figure 2.6: Stages involved in application of LTSM

In the first stage, green field ground movements are computed. Green field movements can be computed using empirical [2] [18] [7], analytical [19] and numerical techniques. Presence of building is not considered in this stage. Some threshold values can be respected at this stage to avoid unnecessary calculations, e.g. to only consider part of building located within influence area of 1 mm settlement value [20]; part of building outside this area is expected to be risk free. Other values, mentioned in literature, are slope of deflection curve and maximum settlement experienced by building [8].

In the second stage, building within the influence area is divided into hogging and sagging zones at the point of inflection (Figure 2.7). Parameters influencing building behavior are calculated for hogging and sagging zones (Figure 2.7).

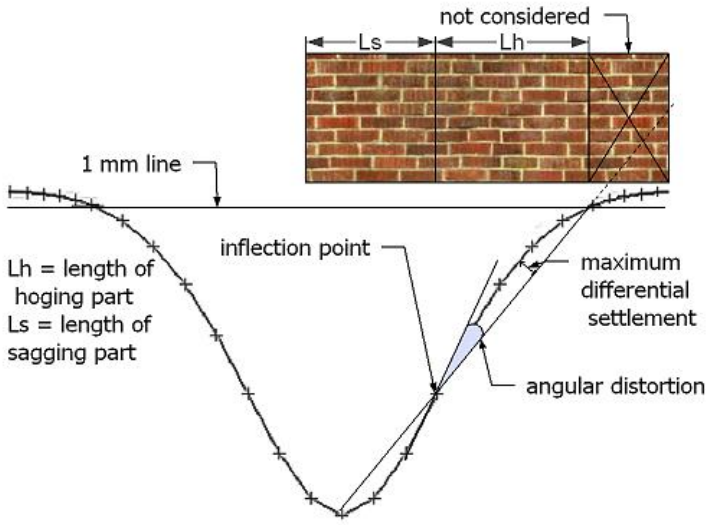

Figure 2.7: Division of wall into hogging and sagging parts

Tensile strains are computed in third stage. Wall is represented as weightless, linear elastic, isotropic, homogeneous, simply supported and rectangular beam of unit thickness. While computing tensile strains, both deformation modes -bending and shear- are considered [14]. Following equations are used for computing bending and diagonal strains:

$$\in_{bmax} = \frac{DR}{\left(\frac{L}{12t} + \frac{3I}{2\,.\,t.\,L\,.\,H}\,.\,\frac{E}{G}\right)} \tag{2.9}$$

$$\in_{dmax} = \frac{DR}{\left(1 + \frac{HL^2}{18\,.\,I}\,.\,\frac{G}{E}\right)} \tag{2.10}$$

Where

L = length of part under consideration, hogging or sagging;
H = height of building;
t = distance of farthest fiber from neutral axis;
I = beam's moment of inertia;
E = modulus if elasticity;
G = shear modulus;
DR= deflection ration

While deriving equations 2.9 and 2.10, value of 0.3 was used as Poisson's ratio. Equation 2.9 and 2.10 corresponds to an imaginary point load in center of beam that will produce same deflection ratio in beam as experienced in greenfield ground movements. Similar equations can be derived for distributed loading but these are not sensitive to loading [14].

Burland and Wroth 1974 assumed neutral axis to be at the base of wall for hogging part, while neutral axis was assumed to be at mid height for sagging part. They reasoned [14], [15] that the foundation soil will offer restraint to deformation and top of wall will be free to deform in hogging zone. Burland and Wroth (1974) also stated that hogging part is more susceptible to damage than sagging part. It is clear form Figure 2.8 that bending strains are critical for L/H more than 0.5, while shear strain dominates lower values of L/H.

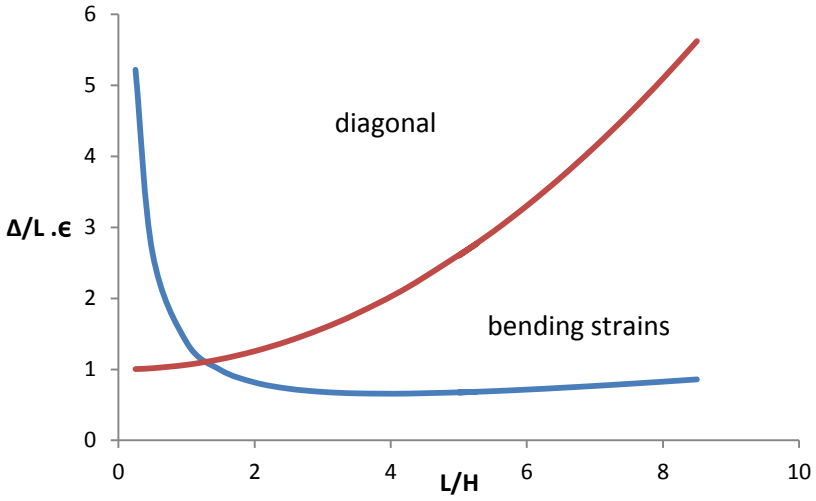

Figure 2.8: Effect of slenderness on bending and shear contribution [14]

Boscardian and Cording (1989) noted that horizontal strain is a substantial component of total tensile strain experience by building, subjected to ground movements related to mining, tunneling and open excavation [15]. Hence, they proposed to add horizontal strain in equations 2.9 and 2.10. Horizontal tensile strains were superimposed on bending tensile strains, while diagonal strains cannot be added directly in horizontal strains. Contribution from diagonal strains was computed using Mohr's circle for strain. Hence, total bending or diagonal strain is:

$$\in_{bt} = \in_{h} + \in_{bmax} \tag{2.11}$$

$$\in_{dt} = 0.35 \in_{h} + \sqrt{(0.65 \in_{h})^2 + \in_{dmax}} \tag{2.12}$$

Total tensile strain, experienced by building, is maximum of the values given by equation 2.11 and 2.12.

After estimation of total tensile strain, a damage classification is assigned to building, which is based on the work of Burland et. al. (1977) [17]. They proposed a classification based on ease of repairing. Boscardian and Cording (1989) assigned range of tensile strains to different levels of damage, defined by Burland et. al. (1977). Table 2.1 shows the proposed classification.

Boscardian and Cording (1989) expressed tensile strains in terms of angular distortion instead of deflection ratios; deflection ratio was used by Burland and Wroth (1974). They [15] also developed a design chart in which horizontal strain was plotted against angular distortion, see Figure 2.9. The design chart, Figure 2.9, was developed for hogging zone. In this design chart, each curved line represents a boundary between two damage zones. The chart also includes field data from tunnel construction, mines and braced cuts.

Similar type of chart was developed by Burland (1995) for hogging zone, using LSTM equations. He [21] developed chart in which deflection ratio was plotted against horizontal strain, using L/H equal to 1 and E/G equal to 2.6, see Figure 2.10.

Table 2.1: Damage classification for masonry [17], [15]

Category of risk of damage	Degree of severity	Description of typical damage	Crack width (mm)	Limiting tensile strain %
0 aesthetic	negligible	Hairline cracks	<0.1	0-0.05
1 aesthetic	Very slight	Fine cracks which are easily treated during normal decoration. Damage generally restricted to internal wall finishes. Close inspection may reveal some cracks in external brick work or masonry.	<1	0.05-0.075
2 aesthetic	slight	Cracks easily filled. Redecoration probably required. Recurrent can be masked by suitable linings. Cracks can be visible externally and some repointing may be required to ensure water tightness. Doors and windows may stick slightly.	<5	0.075-0.15
3 aesthetic/ functional	Moderate	The cracks require some opening up and can be patched by a mason. Repointing of external brickwork and possibly a small amount of brickwork to be replaced. Doors and windows sticking. Service pipes may fracture. Water tightness often impaired.	5 -15 many cracks >3 mm	0.15-0.3
4 functional/ serviceability	severe	Extensive repair work involved breaking out and replacing sections of walls, especially over doors and windows. Windows and door frames distorted, floor sloping noticeably. Walls leaning or bulging noticeably, some loss of bearing in beams. Service pipes disrupted.	15-15 depends on number of cracks	>0.3
5 structural	Very severe	Major repairing job involving partial or complete rebuilding. Beams loose bearing. Walls lean badly and requiring shoring. Windows broken with distortion. Danger of instability	>25 Depends on number of cracks	

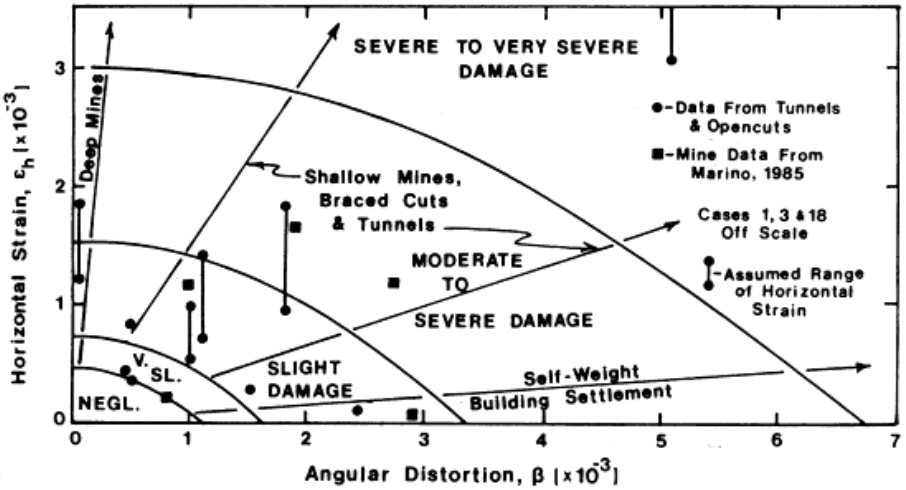

Figure 2.9: Design chart developed by Boscardian and Cording, 1989 (L/H =1, E/G =2.6)

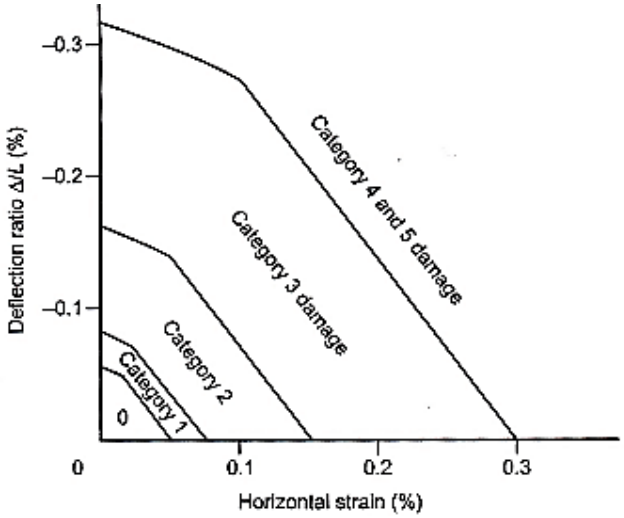

Figure 2.10: Design chart developed by Burland, 1995 [21]

2.4.2. Modifications in Limiting Tensile Strength method(LSTM)

The LTSM approach, discussed above, is a very rudimentary and conservative way of estimating tunnel-related damage in existing building. The method does not take into account the effect of building's stiffness, relative movement between soil and building's foundation, presence of openings in wall, non-linearity of material and effect of superimposed loads; all of which have a significant effect on tunnel-related damage [22], [23], [24], [25], [26]. This section reviews some of the improvements proposed for LSTM method.

2.4.2.1 Relative Stiffness approach: Potts and Addenbrooke, 1997

Potts and Addenbrooke(1997) conducted a 2D finite element study and proposed a set of charts to modify the greenfield(GF) movements, taking into account the effect of building's stiffness. They represented building as a weightless, elastic and isotropic beam, rigidly connected to soil. Over 100 plane strain models were analyzed, considering eccentricity of building with respect to center-line of tunnel; modification factors were computed to modify greenfield ground movements, such as deflection ration and horizontal strain, and design charts. Figure 2.11-2.12, were developed to correlate modification factors to axial and bending stiffness of building.

They [25] defined following modification factors for sagging and hogging:

$$M^{DR_{sag}} = \frac{DR_{sag}}{DR_{sag}^{GF}} \tag{2.13}$$

$$M^{DR_{hog}} = \frac{DR_{hog}}{DR_{hog}^{GF}} \tag{2.14}$$

And following modification factors for maximum horizontal tensile and compressive strains:

$$M^{\epsilon_{ht}} = \frac{\epsilon_{ht}}{\epsilon_{ht}^{GF}} \tag{2.15}$$

$$M^{\epsilon_{hc}} = \frac{\epsilon_{hc}}{\epsilon_{hc}^{GF}} \tag{2.16}$$

It can be noted that Potts and Addenbrooke(1997) [25] used maximum tensile and compressive strains instead of average values, which were used by Burland and Wroth(1974) [14]. In equations 2.15 and 2.16, subscripts *hc* and *ht* denotes horizontal compressive and horizontal tensile.

Potts and Addenbrooke(1997) used following relation to define relative bending and axial stiffness of building:

$$\rho^* = \frac{EI}{E_s(B/2)^4} \quad (2.17)$$

$$a^* = \frac{EA}{E_s(B/2)} \quad (2.18)$$

In equations, 2.17 and 2.18, E_s is secant modulus of soil corresponding to 0.01% axial strain in triaxial compression test, performed on a sample taken from half of tunnel depth; *B* is dimension of building perpendicular to axis of tunnel; *EI* and *EA* are bending and axial stiffness of building, respectively.

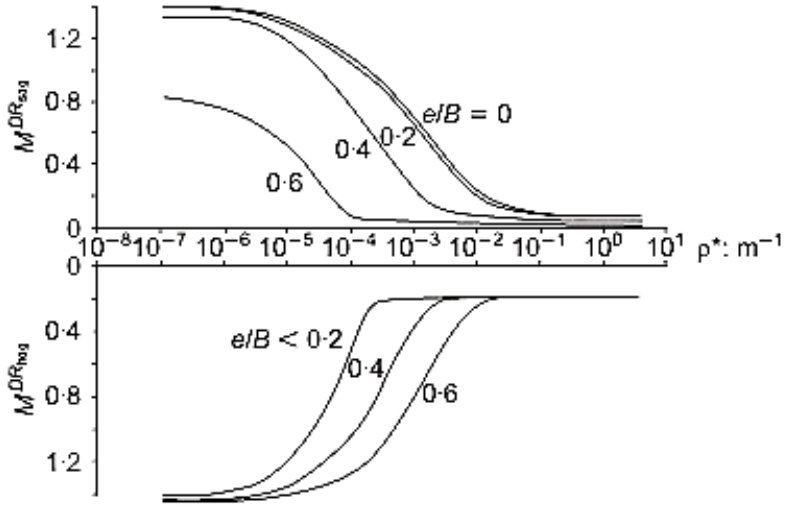

Figure 2.11: Chart to modify greenfield deflection ratios

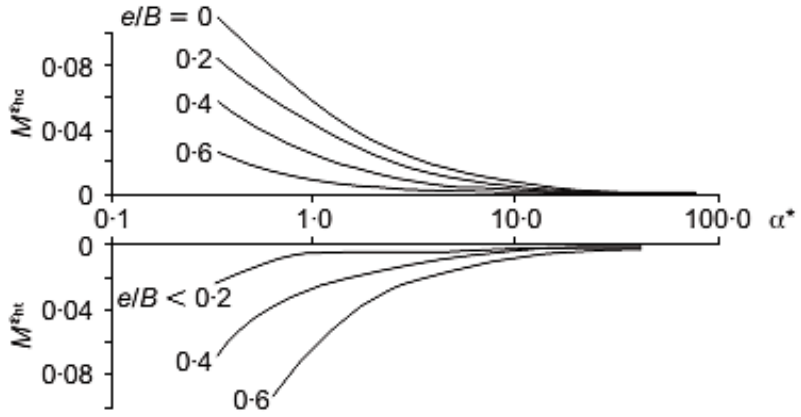

Figure 2.12: Chart to modify greenfield horizontal strains

2.4.2.2 Modified Relative Stiffness approach: Franzius et al., 2006

Franzius et al.(2006) [22] conducted a numerical study in which they included wider variation of building geometry and tunnel depths as compared to the study of Potts and Addenbrooke(1997) [25]. They also investigated the effect of weight of building, soil-structure interface and the 3D effects of building on the modification factors, proposed earlier by Potts and Addenbrooke(1997).

They concluded that the weight, soil-structure interface and length on building, parallel to tunnel axis, has insignificant effect on modification factors of Potts and Addenbrooke(1997).

The results of their study [22] showed that the effect of B (building's length perpendicular to tunnel axis) was overestimated, while depth of tunnel was not appropriately accounted for in original relative stiffness values of Potts and Addenbrooke(1997). They realized that the inclusion of building's length (parallel to tunnel axis) in expressions of relative stiffness will lead to a dimensionless value.

They proposed following modified expressions for relative bending and axial stiffness of building:

$$\rho^*_{mod} = \frac{EI}{E_s \,.\, Z_o \,.\, (B)^2 \,.\, L} \qquad (2.19)$$

$$a^*_{mod} = \frac{EA}{E_s \,.\, B \,.\, L} \qquad (2.20)$$

The figure 2.13 shows design curves for modification of deflection ratio, taking into the account the modified values of relative bending stiffness of building.

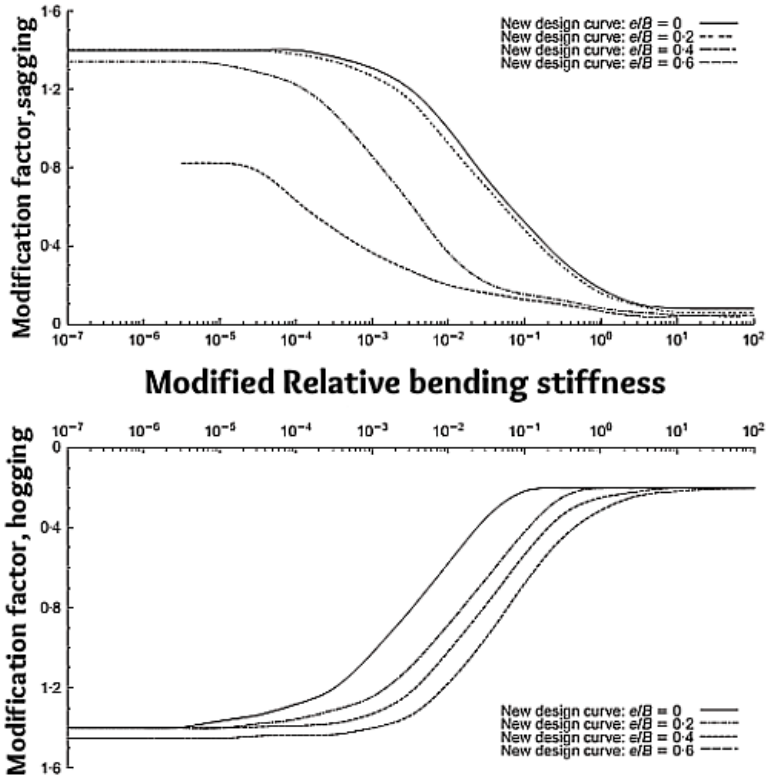

Figure 2.13: Modified design curves for deflection ratios, after Franzius et al. [22]

2.4.2.3 Netzel's (2009) modifications

Original LTSM method was reviewed by Netzel [24] in 2009, and he concluded:

- In original LSTM, shear form factor of 1.5 was used, which overestimates the contribution of shear deflection and underestimates tensile strains. He recommended to use value of 1.2, which can increase strains up to 25% [24].

- It is common practice to divide building over point of inflection into hogging and sagging zones. He [24] showed that the practice can underestimate damage if tilt of total building differs by more than 15% to tilt of separated parts. Therefore he recommended that the beam model of building should not be separated into different parts if difference in tilt is more than 15%, and additional numerical calculations are required in that case. Similarly, he recommended including the part of building that is beyond the 1mm settlement line.
- In original LTSM, Burland and Wroth (1974) used deflection ratio, while Boscardian and Cording (1989) used angular distortion to quantify differential vertical movements of ground. He recommended using angular distortion for computing diagonal strains, and deflection ratio for computing bending strains; he [24] showed that other procedures can under- or overestimate damage.

2.4.3. Strain Superposition Method

Boone (2001) [27] used similar approach, the one employed by Burland (1974) [14] and Boscardian and Cording (1989) [15], to evaluate the risk of damage posed by tunnel-related ground movements. He represented building by uniformly loaded deep beam, instead of a beam loaded by point load; neutral axis was assumed to be located at mid height for hogging, not at bottom of wall. The reader is directed to [27] for further reading.

Chapter 3

Method of Analysis

3.1. Overview

As discussed earlier, construction of microtunnels, required for innovative base-isolation technique [1], will induce ground movements that can damage the building. Hence, it is very important to ascertain the damage associated with construction of these closely-spaced microtunnels in various soil conditions, and to walls of various physical and mechanical characteristics. This will establish suitability of innovative base-isolation technique.

In this work, only the effect of transverse ground movements is considered. The suitability of innovative base-isolation technique has been investigated by changing mechanical properties of masonry wall of particular geometric properties and subjecting it to tunneling in soil of varying stiffness' so as to obtain damage levels that will effects its aesthetics. A nonlinear, 2D and coupled finite element analysis has been done.

To cater for walls of different geometric characteristics, their length, height, as well as opening configuration has been varied in this study. Four lengths are chosen: 12.5m, 15.5m, 20m and 22m; height of wall is chosen in two different ways, representing a two story and four story building. For a wall of particular length and height, three different opening configurations are considered,

along with a case of wall without any opening. Three opening configurations are: wall having openings for door and windows, with door located at center of wall; wall having only window openings; wall having openings for door and windows, with door located away from center. Figure 3.1 to 3.4 shows opening configurations of two story walls for 12.5m, 15.5m, 20 and 22m long wall.

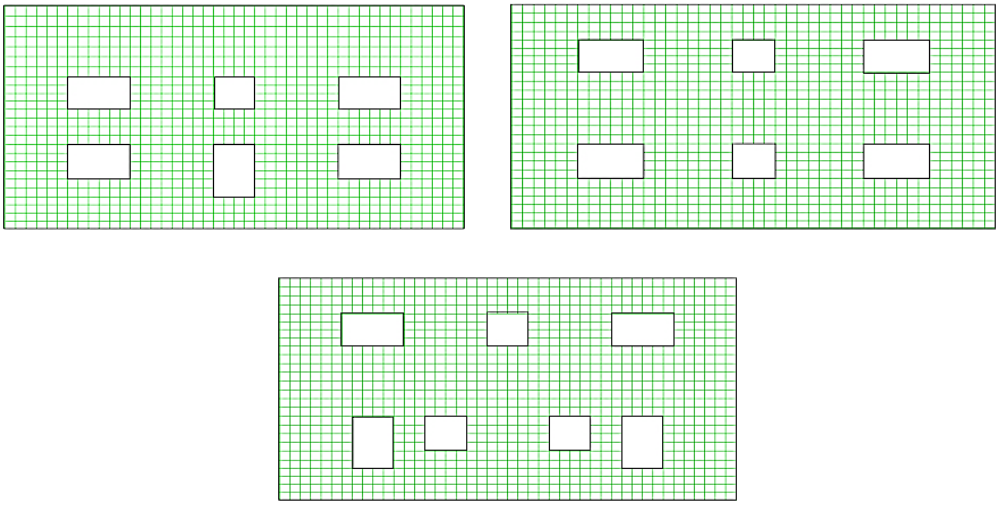

Figure 3.1:opening configurations for 12.5m wall

The diameter of each micro-tunnels is chosen as 2m so that they can be easily assessed for installation of isolation devices. As discussed earlier, tunnels are closely spaced: the isolation devices will be fitted in the wall of two adjoining linings of micro-tunnels; the distance between centerlines of microtunnels is kept at 2.2m in this numerical study. Consequently, 6 tunnels are required to isolate wall of 12.5m length, 7 for 15.5m, 9 for 20m, and 10 tunnels are required for 22m long wall.

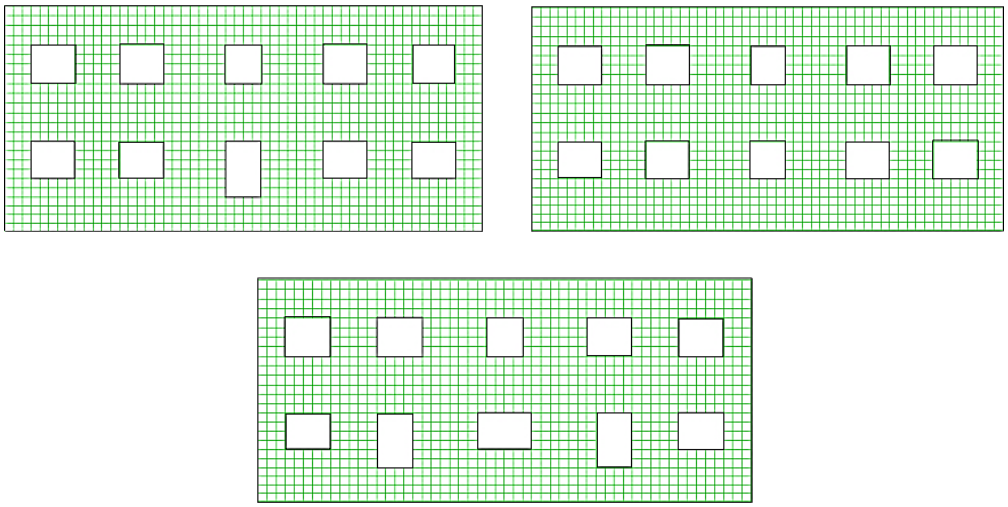

Figure 3.2: opening configurations for 15.5m wall

The sequence of excavation of micro-tunnels affects the damage sustained by masonry wall [26]. Various sequences of tunnel excavation were investigated for each set of microtunnels, see Figure 3.5-3.8, so as to find the one, inflicting minimum damage, on masonry wall. Three excavation sequences have been considered for wall isolated with assembly of six tunnels, six excavation sequences for wall isolated with assembly of seven tunnels, eight excavation sequences for wall isolated with assembly of nine tunnels, and five for wall isolated with assembly of ten tunnels.

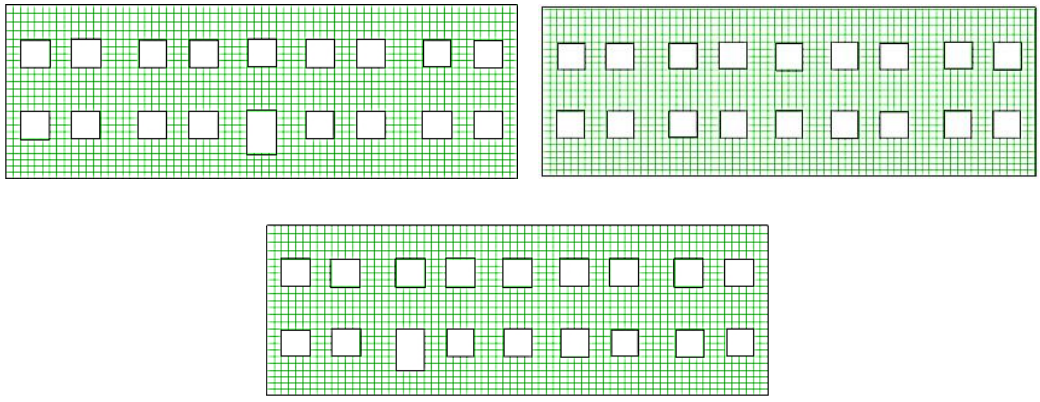

Figure 3.3:opening configurations for 20m wall

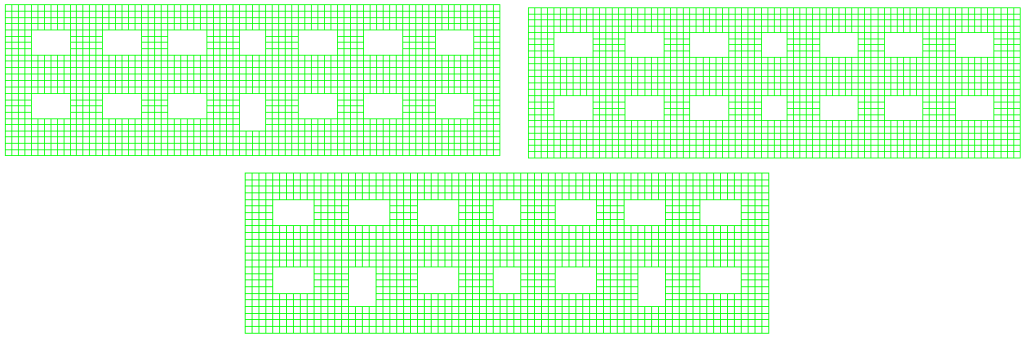

Figure 3.4:opening configurations for 22m wall

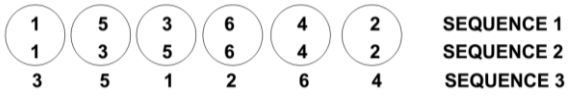

Figure 3.5: sequence of excavation considered for set of 6 tunnels

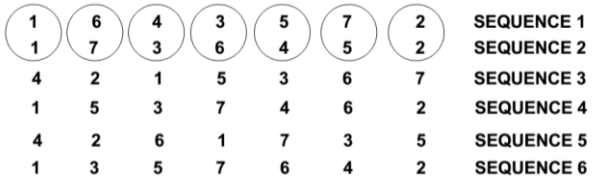

Figure 3.6: sequence of excavation considered for set of 7 tunnels

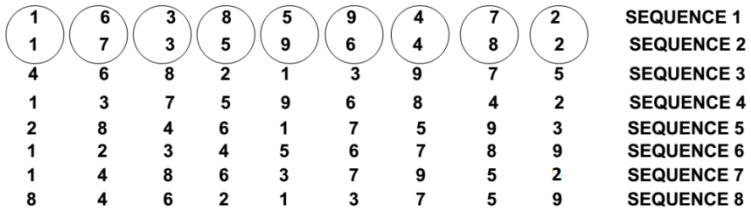

Figure 3.7: sequence of excavation considered for set of 9 tunnels

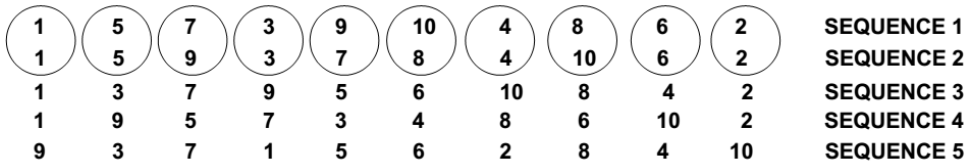

Figure 3.8: sequence of excavation considered for set of 10 tunnels

3.2. Finite Element Model

As discussed earlier, coupled approach has been adopted: soil and masonry has been modeled together. Interface has been inserted between soil and masonry to simulate relative tangential movements between masonry and soil; two types of interface has been used: one allows tangential movements at small tangential stresses(smooth interface), and the other does not allow tangential movements at small tangential stresses (rough interface).

Soil has been discretized using eight-noded quadrilateral plane-strain elements, masonry by eight-noded quadrilateral plane-stress elements, interface by six noded line-interface element,

lining by three noded curved shell elements and lintel by three noded 2D beam element. 3x3 integration scheme has been adopted for masonry elements; 5-point lobatto integration scheme for interface elements.

The diameter of tunnel is chosen as 2m so that tunnels are accessible, and distance between their centres is 2.2m. Depth of tunnel construction is chosen as 6m; it was also varied during study for comparison purposes.

The bottom and side boundaries of soil are constrained in perpendicular direction. The bottom boundary is kept at 8D from centre of tunnels; side boundary is also kept at 8D from centre of outermost tunnel.

The model is loaded with gravity as well as superimposed service loads (about 7.5 kN/m), acting on floor levels. In order to simplify the problem, dampers are not included in the model.

The Figure 3.9 shows the meshed model, involving 22m long wall with door opening at centre.

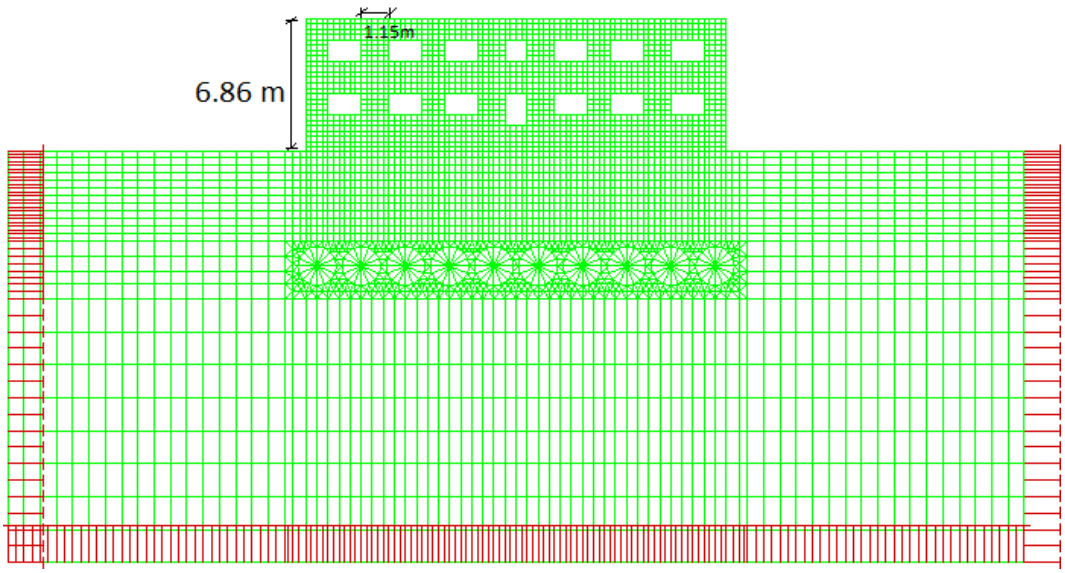

Figure 3.9: coupled model, 22 m long wall with 10-tunnel assembly

3.2.1. Excavation simulation

Simulation of sequential tunnelling obeys the following procedure. Initial soil stresses are established first, which are based on unit weight of soil and coefficient of earth pressure at rest; displacements are suppressed in this phase. Next step involves activation of masonry, lintel and interface elements along with their self-weight and superimposed loads. The model attains new equilibrium state . Excavation starts from third step; the excavation process is simulated as:

- Soil elements, corresponding to the first tunnel, are removed, and model is allowed to establish equilibrium under gravity and superimposed loads; DIANA's 'phased analysis' is used for this purpose [28]. No internal pressure is applied on the periphery of excavation.
- In the next phase, soil elements, corresponding to the second tunnel, are removed; lining elements are added around the first tunnel and model is allowed to establish equilibrium under gravity and superimposed loads. No internal pressure is applied on the periphery of the excavation.
- The previous step is repeated for the remaining tunnels.

In the above steps, it is assumed that the "annular space" or the "gap" (i.e. the space left between excavated soil and lining) is the main source of volume loss, owing to the chosen material properties of soil, depth of construction, and size and alignment of tunnels. Volume loss is simulated by allowing the tunnel to undergo instantaneous settlement, with no pressure applied on excavated boundary, before the installation of lining elements. Since the introduction of the lining elements into the model prevents further closure of the gap, the remaining gap must be completely filled with grout after installation of lining during actual construction process.

3.3. Constitutive laws for materials and their properties

Masonry has been modelled as elastic softening material. It is modelled as a homogeneous, isotropic and linear-elastic material in elastic regime; smeared crack approach with strain decomposition is used to simulate its fracturing process. Fixed-crack model with linear tension softening and constant tension cut-off criteria([29]; [30]) is used to simulate crack initiation and propagation, see Figure 3.10.

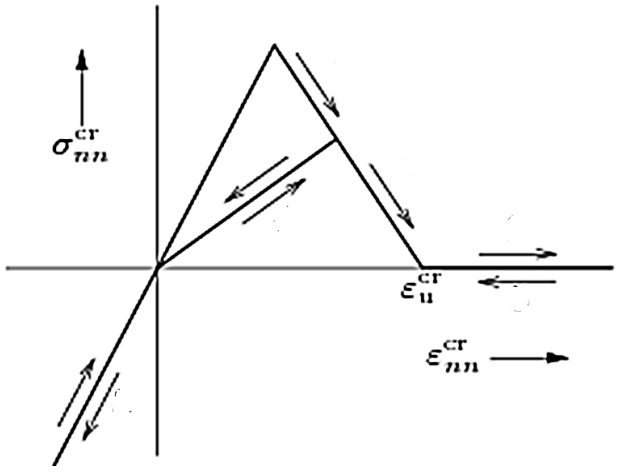

Figure 3.10: constitutive law for masonry

Five different mechanical properties of masonry have been used in this study to represent different conditions of historical masonry, see Table 3.1. These numbers have been taken from literature. The thickness of wall is chosen as 0.22m during the study.

Soil is modelled as a homogeneous, isotropic, linear-elastic perfectly-plastic material with Mohr-Coulomb yield surface and zero-tension cut-off. The mechanical properties, representing strength of soil, have been kept constant throughout the study, while the stiffness of soil, represented by its elastic modulus, is varied (Table 3.2).

Table 3.1: material properties for masonry

Material ID	Em (GPa)	F_t (kPa)	G_f (N/m)	h (m)	γ (kN/m^3)	β(-)	ν (-)
MSN3	3	150	45	0.28	20.5	0.01	0.2
MSN4	4	200	45	0.28	20.5	0.01	0.2
MSN5	5	250	45	0.28	20.5	0.01	0.2
MSN6	6	300	50	0.28	20.5	0.01	0.2
MSN8	8	350	50	0.28	20.5	0.01	0.2

Table 3.2: material properties for soil

E (MPa)	c(kPa)	γ (kN/m^3)	ν (-)	Ψ (°)	ϕ (°)	K_o (-)
variable	80	17.5	0.3	0	13	0.47

In the table 3.1 and table 3.2, Em: elastic modulus of masonry; E: elastic modulus of soil; Ft: tensile strength; G_f : fracture energy; h: crack band width; β: shear retention factor; γ: unit weight; ν : Poisson's ratio; c: cohesive strength; Ko: coefficient of lateral earth pressure at rest; ϕ: angle of friction: Ψ is dilatancy angle.

The interaction between soil and masonry is modelled using interface elements, relating normal(σ) and shear forces(τ) to normal(Δu_t) and shear(Δu_n) relative displacements across the interface. The behaviour of interface is simulated in two ways, as discussed earlier. The Coulomb friction model with gap criteria is used to simulate slip and gap for rough interface; friction behaviour is not considered for smooth interface, see Figure 3.11. The normal (k_n) and tangential stiffness for smooth interface are chosen as 4 x 10^8 N/m3 and 5 N/m3, respectively. For rough interface, normal and tangential stiffness is chosen as 4 x 10^8 N/m3 and 4 x 10^7 N/m3, respectively, friction angle is 20° and tensile strength is zero.

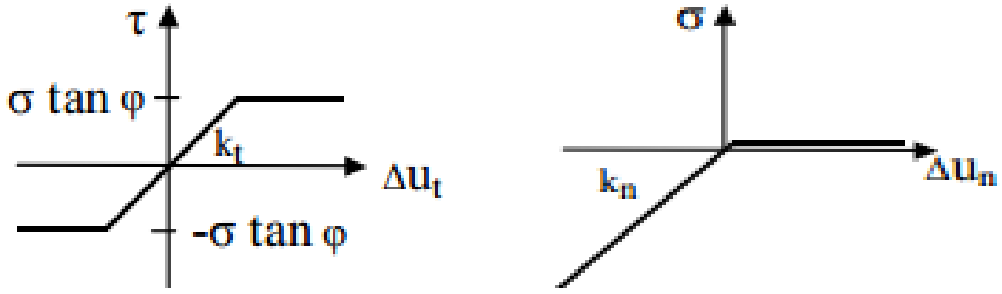

Figure 3.11: constitutive law for rough interface

The lining and the lintel is modelled as a linear-elastic, isotropic and homogeneous material; Uniform thickness of 0.1m is selected for lining, and its elastic modulus is kept at 21GPa. The size of lintel is 0.22m x 0.22m and its elastic modulus is 15GPa.

Chapter 4

Results and Discussion

This section will present the results of the finite element study. Damage, sustained by masonry due to excavation of closely-spaced microtunnels, has been defined in terms of maximum crack width in principle direction. Damage reported in the figures is the one obtained after excavation simulation of all tunnels, unless mentioned otherwise. Results are plotted in terms two levels of damage: 1mm and 2.5mm crack width; these values of damage does not harm the ability of building to function in an intended way.

Results are presented in terms of: maximum crack width in principle direction- denoted by 'crack', or 'crack width' in figures-; distribution of cracks; average horizontal tensile strain at bottom of masonry- computed as ratio of change in length to the length of wall; volume loss, computed by integrating transverse settlement profile; interface stresses and deflection ratio. In section 4.8, some additional results, discussed later, are also shown.

Bubble and scatter charts have been presented in each section. In bubble chart, each bubble is accumulation of three data points, corresponding to three opening configurations. Mechanical properties, defined in Table 1 and Table 2, of soil and masonry are plotted on the axes of these bubble charts. In scatter chart, each data point shows mechanical properties of soil and masonry, required to limit the damage to a particular level for a wall of a particular opening configuration.

The results presented in figures correspond to an excavation sequence that leads to least damage, unless mentioned otherwise.

In the figures, shown in this section, 'central door' refers to an opening configuration consisting of door and windows with door located at centre of wall; 'window' refers to an opening configuration consisting of only windows; and 'door off-centre' refers to an opening configuration consisting of door and windows with door located away from the centre of wall.

4.1. Wall isolated with 6-tunnel assembly

4.1.1. Smooth interface

For this wall, 'excavation sequence 1' (see section 3.1) induced least damage on wall for all opening configurations.

The Figure 4.1 shows a bubble chart. The graph shows that the stiffer/stronger conditions of soil and masonry are required to keep the damage at particular level for taller walls as compared to shorter walls. Hence the effect of weight of building outweighs the effect of increased stiffness of wall due to its height.

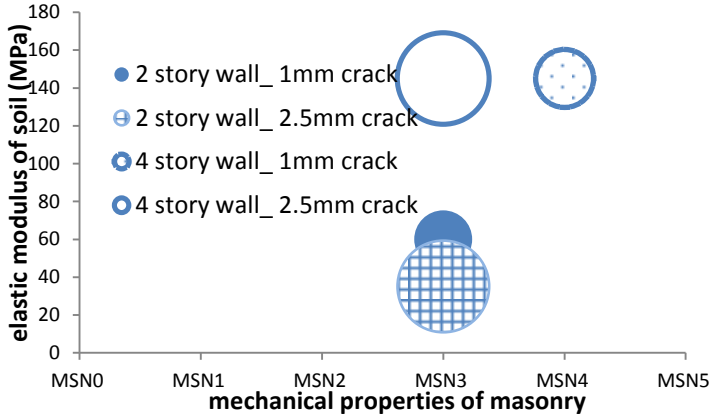

Figure 4.1: mechanical properties of masonry and soil for different damage levels

The Figure 4.2 and 4.3 shows results in scatter form; Each data point shows mechanical properties of soil and masonry, required to limit the damage level, defined in terms of maximum crack width, to a particular level for a wall of a particular opening configuration.

The Figure 4.2 shows the applicability of the innovative base isolation technique in a variety of soil conditions for a wide range of masonry conditions, especially if the damage criterion is lenient.

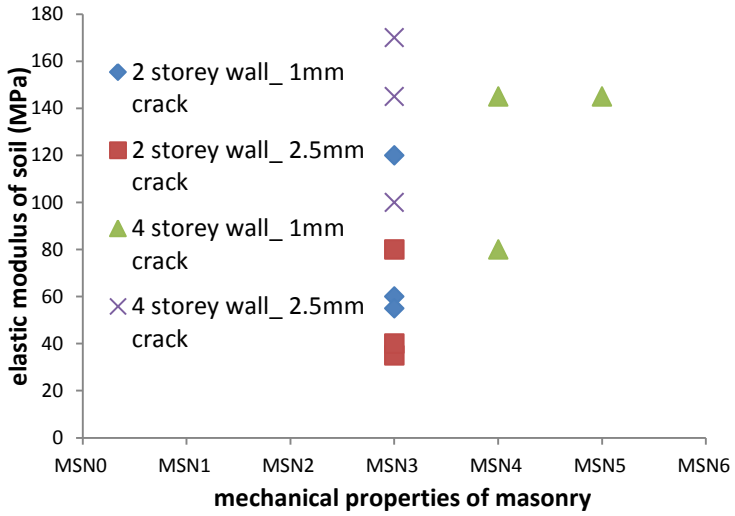

Figure 4.2: mechanical properties of masonry and soil for different damage levels (scatter)

The results, in Figure 4.3, show that the wall, supporting door opening in the central region, will sustain most damage for given conditions of soil and masonry; wall, without openings, will sustain least, or negligible, damage. Figure 4.3 does not show results for 4-story wall, to reduce clutter.

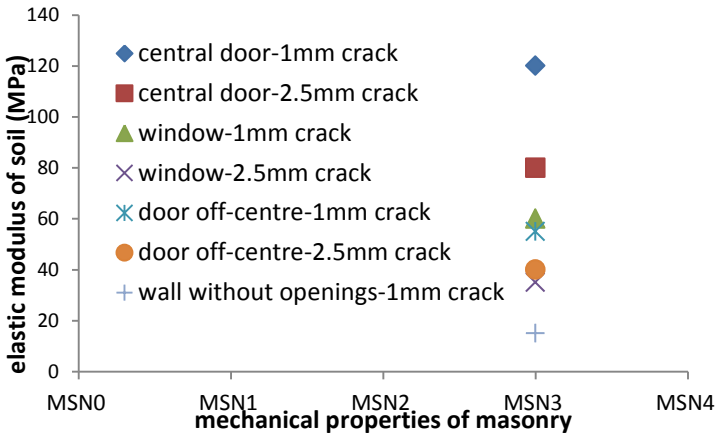

Figure 4.3: effect of opening configuration on damage susceptibility, 2 story wall

In Figure 4.4-4.7, maximum crack width, volume loss, average horizontal tensile strain and deflection ratio has been plotted against excavation stages. The results for 4, as well 2, story wall have been shown for an opening configuration consisting of central door, along with results of 4 - story wall with only window openings. The results show that weight of the wall has a significant effect on tunneling induced ground movements, and hence on damage.

Figure 4.4 show that the volume loss for the last tunnel will be much more than the volume loss encountered for first tunnel, showing the effect of interaction between close tunnels. This study assumed that the annular space is the main source of volume loss, and that the remaining annular space-after excavation of each tunnel- will be filled with grout; hence, heavier wall will lead to more closure of annular space than lighter wall.

Figure 4.5 shows that the wall will experience more horizontal tensile stresses as the excavation process will proceed. The result also shows the effect of opening configuration on damage susceptibility of wall; the wall, supporting door opening in central region, will sustain more damage than the wall consisting of only windows. As mentioned earlier, weight of wall, and superimposed loads, has a significant effect on tunneling induced ground movements.

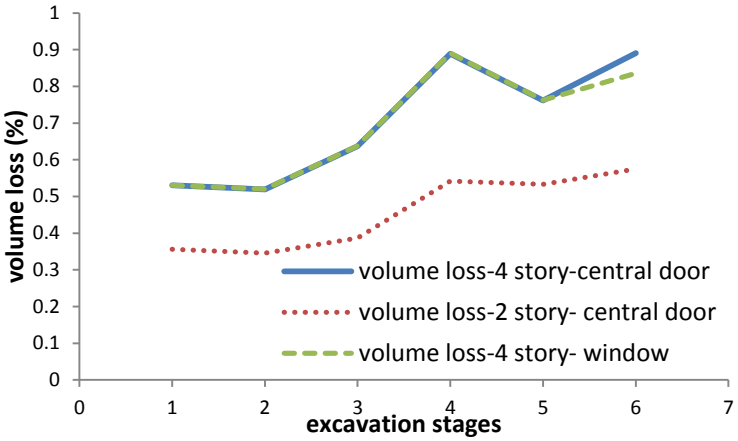

Figure 4.4 : volume loss after each excavation

Figure 4.6 and 4.7 show that the increase in stiffness of wall, due to height, have not overcome the effect of increase in loading for taller wall, and consequently lead to more deflection ratio and damage; reason being: volume loss will also increased with increase in weight.

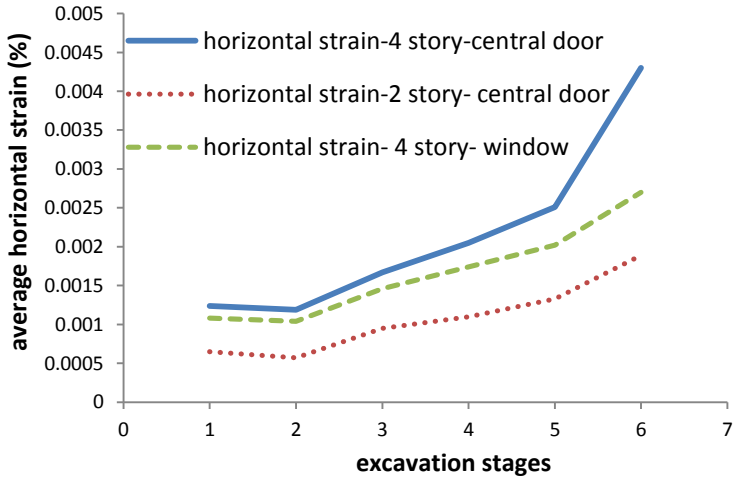

Figure 4.5: average horizontal tensile strain after each excavation stages

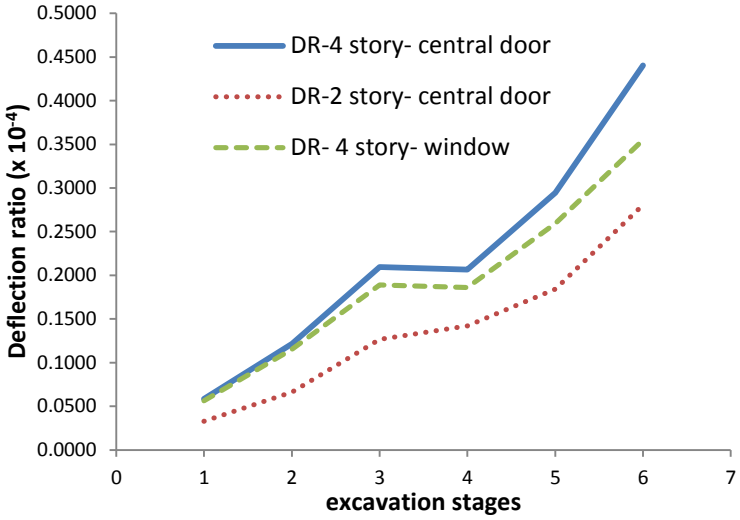

Figure 4.6: Deflection ratio after each excavation stage

The distribution of normal interface stresses in central region of wall, consisting of openings for only windows, is different than the wall supporting an opening configuration, dubbed as 'central door'. The presence of door reduces the normal interface stresses below the door, thereby increasing normal interface stresses around the door, when compared to the normal interface stresses for wall with only window openings. This- somewhat abrupt- change in value of differential stresses around the door opening leads to abrupt change in differential vertical movements around door opening as compared to other opening configurations. The Figure 4.8 compares the snapshot of vertical interface stresses for two opening configurations.

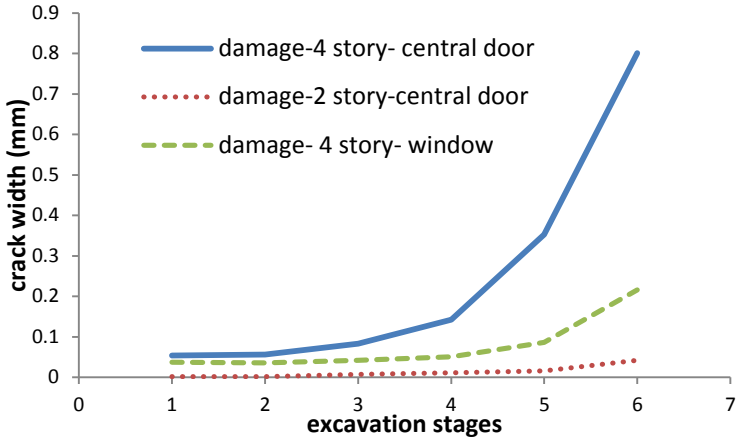

Figure 4.7: maximum crack width after each excavation stage

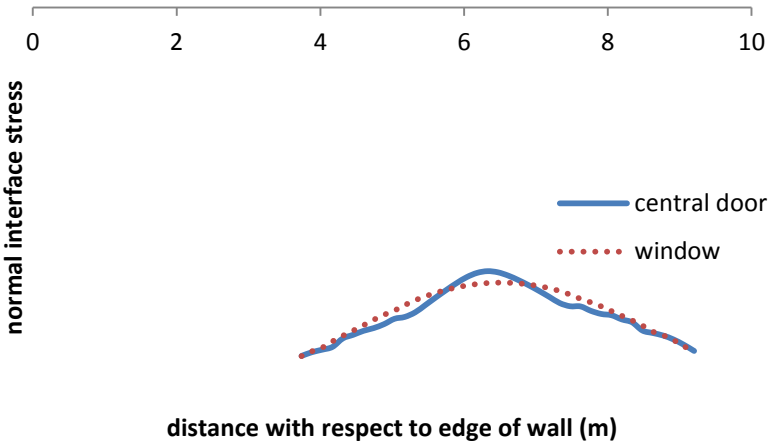

Figure 4.8: snapshot of vertical interface stresses at central region of 4 story wall

In this type of tunneling process, entire building will be in the sagging region after the excavation of all tunnels, as tunnel-set covers entire dimension of building. The wall did not

sustain any damage in hogging region during excavation simulation of individual tunnels. Consequently, tunnel related damage will instigate from the bottom region of wall.

4.1.2. Rough interface

The wall without openings sustained no damage for the case of rough interface. Wall (4 as well as 2 story) was subjected to a closely-spaced microtunneling operation in soil having elastic modulus of 30MPa; mechanical properties of wall were assigned as MSN3.

The wall (4 as well as 2 story) with openings, all three opening configuration, sustained negligible/very slight damage -as defined by [17]- when subjected to simulation of closely-spaced microtunnels in soil having elastic modulus of 30MPa; mechanical properties of wall were assigned as MSN3, see earlier sections. The wall sustained damage around openings, see Figure 4.9.

Rough interface has a beneficial effect on wall as it restricts relative movements between soil and foundation in elastic regime, thus inducing compressive stresses in wall.

The wall was analyzed against all three excavation sequences (see section 3.1).

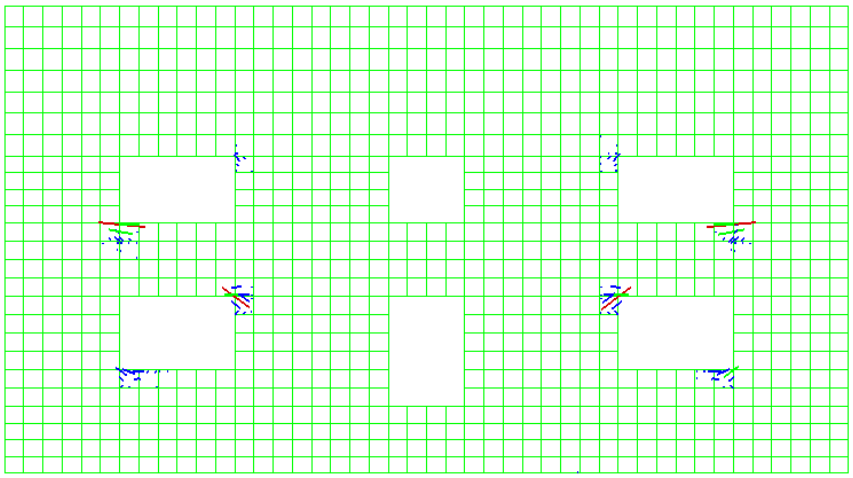

Figure 4.9: crack distribution after last excavation, rough interface

4.2. Wall isolated with 7-tunnel assembly

4.2.1. Smooth interface

For this wall, ‘excavation sequence 4’ (see section 3.1) induced least damage on wall for all opening configurations.

The Figure 4.10 shows a bubble chart. The graph shows that the stiffer and stronger conditions of soil and masonry are required to keep the damage at particular level for heavier walls as compared to lighter walls. Hence the effect of weight of building will outweigh the effect of increased stiffness of wall due to its height; increase in weight can lead to increase in values of deflection ratio and horizontal strains, as discussed in previous section, which will increase the damage. The results show that the applicability of the innovative base isolation reduces as the length of building increases, as bending stiffness has reduced for the same loading conditions. The last claim was made by comparing the results of previous case with this one.

The Figure 4.11 presents the results of Figure 4.10 in scatter chart. One can note the mechanical properties for masonry and soil corresponding to different levels of damage. The right most points, in Figure 4.11, correspond to configuration of 4 story wall, having door openings, showing that for a given length, taller walls with door openings are most susceptible to excavation work required for this innovative base-isolation technique.

The Figure 4.12 emphasizes the role of opening configurations in damage susceptibility of masonry wall to the construction of closely spaced microtunnels. The wall with central door is expected to sustain most damage for a given set of conditions than other opening configurations. The wall with window openings performed much better; the wall, without any openings, is expected to sustain only hair line cracks in most soil conditions.

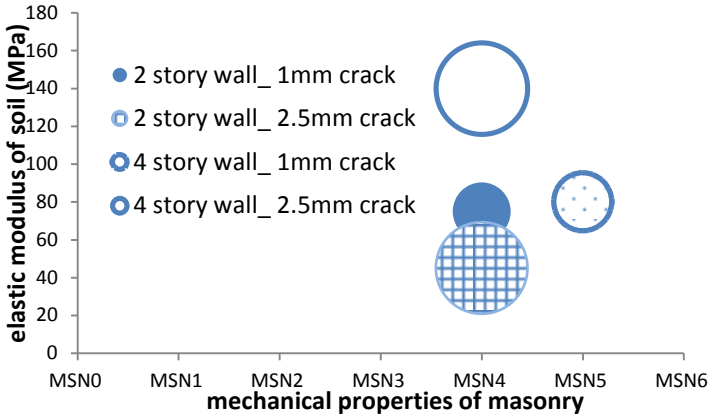

Figure 4.10: mechanical properties of masonry and soil for different damage levels

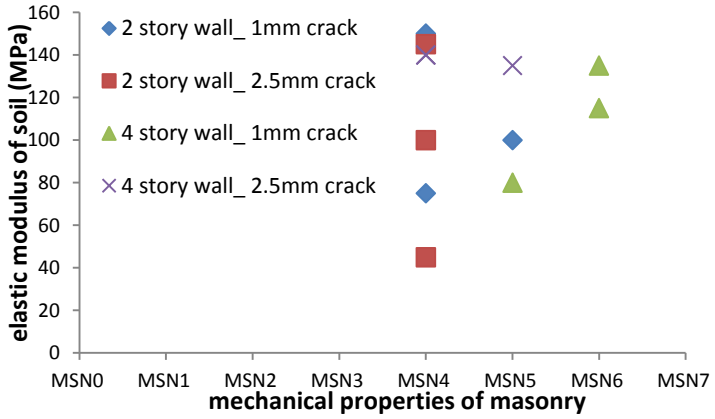

Figure 4.11: mechanical properties of masonry and soil for different damage levels (scatter)

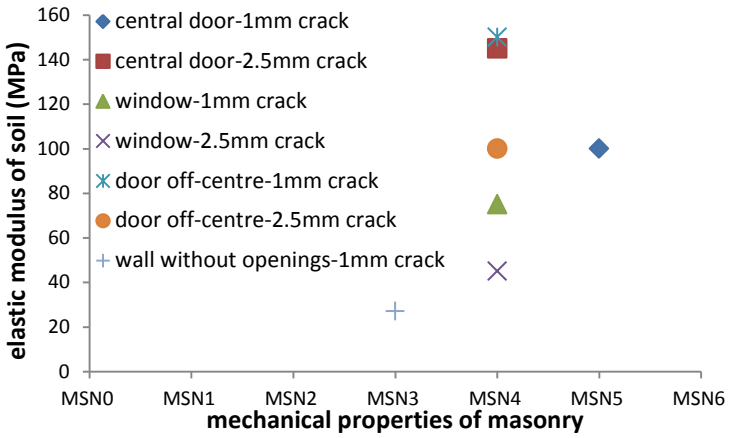

Figure 4.12: effect of opening configuration on damage susceptibility, 2 story wall

Results shows that the entire building will lie in sagging zone after excavation of all tunnels, as excavation covers entire dimension of wall. The results showed that the damage will be accumulated in bottom region of wall, see Figure 4.13. The Figure 4.13 also shows that cracks will propagate in step pattern, breaking the bond between head and bed joints of brick masonry. The cracks are distributed over a wider area for the case of wall without openings (Figure 4.13).

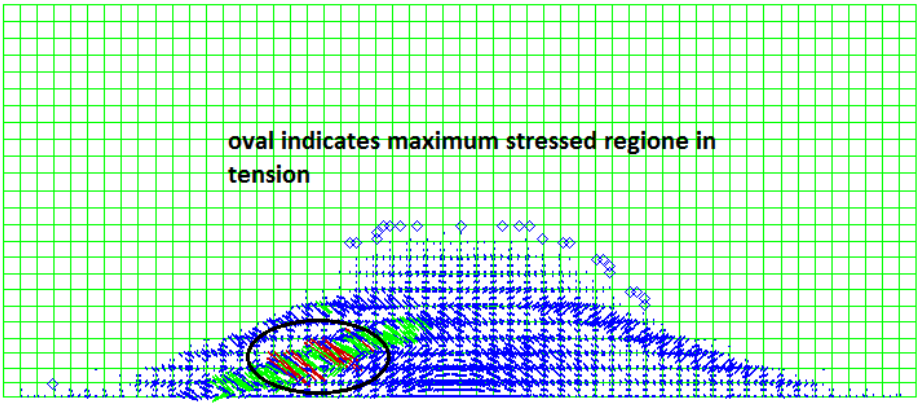

Figure 4.13: distribution of cracks in 2 story wall, without openings, at last excavation stage

Location of maximum damage and distribution of cracks will depend on excavation sequence and opening configuration. The Figure 4.14 and Figure 4.15 shows crack distribution for a wall having opening for door. The damage is located at bottom-center of wall, around door opening, showing the effect of concentration of stresses around door opening. Damage initiated at bottom-center and propagated towards door openings for wall with off-center door. In the case of central door opening, damage initiated at bottom of door opening, as well bottom center of wall, see Figure 4.15, and then propagated towards each other; the hogging experienced by wall during first two excavation stages resulted the initiation of cracks at the bottom of door opening. For both opening configurations, cracks initiated at direction parallel to bottom boundary of wall.

The Figure 4.15b shows crack distribution for a wall having openings for windows, only. In this case, too, cracks initiated from bottom and propagated towards window openings. The cracks are distributed on wider area than for the case of central-door opening.

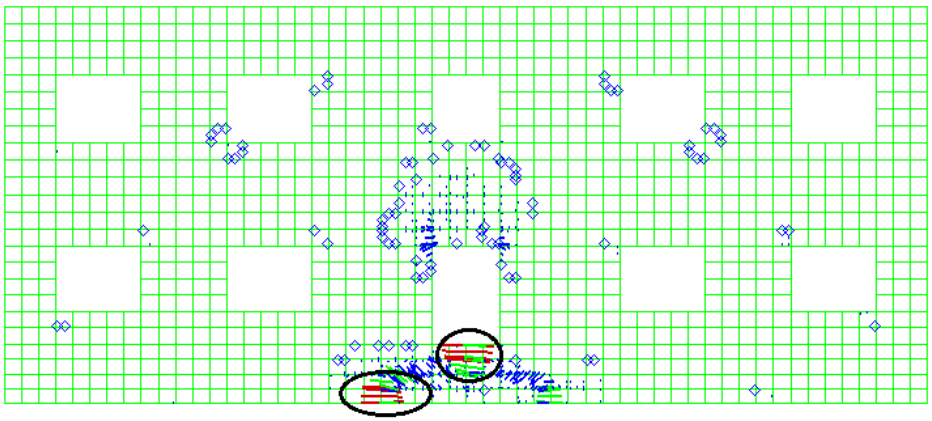

Figure 4.14: distribution of cracks in 2 story wall, central-door opening, at last excavation stage

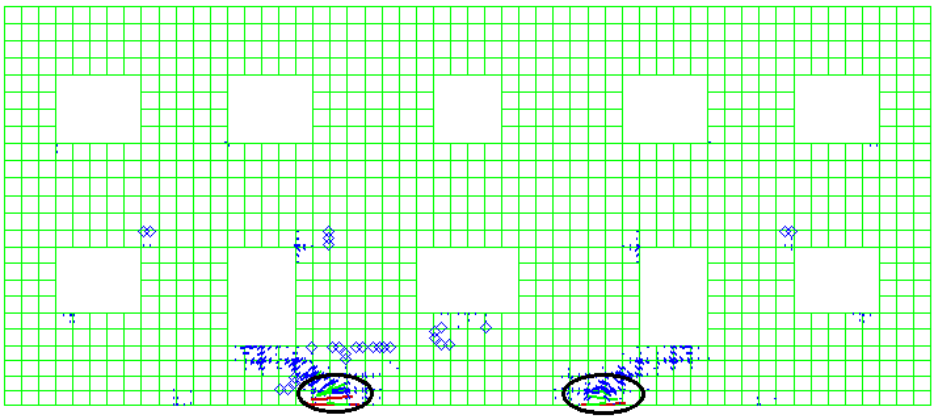

Figure 4.15: distribution of cracks in 2 story wall, door off-center, at last excavation stage

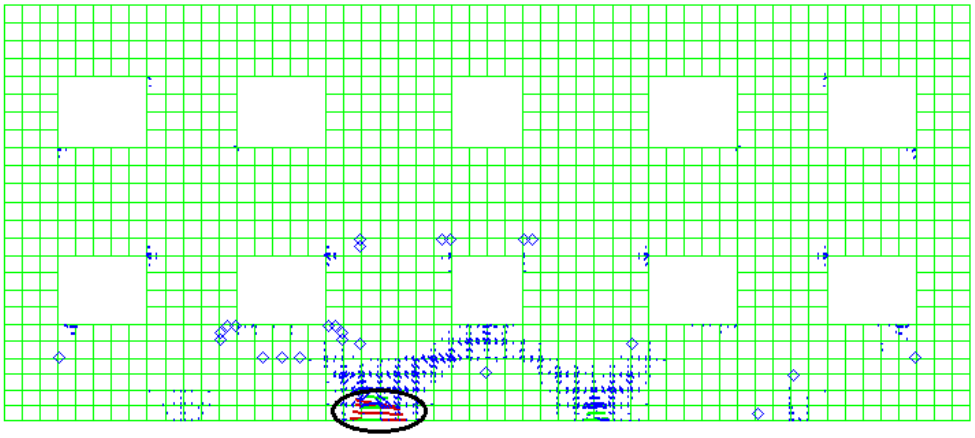

Figure 4.15b: distribution of cracks in 2 story wall, window openings, at last excavation stage

The choice of excavation sequence can have a significant effect on damage sustained by a masonry wall subjected to construction of closely-spaced microtunnels. As shown in Figure 4.16, the Sequence 4 (see Figure 3.5) inflicted minimum damage, while ‘sequence 3’ proved most

harmful. The results also showed that the excavation sequence which is favorable -inflicting minimum damage- for one opening configuration is also favorable for other opening configurations.

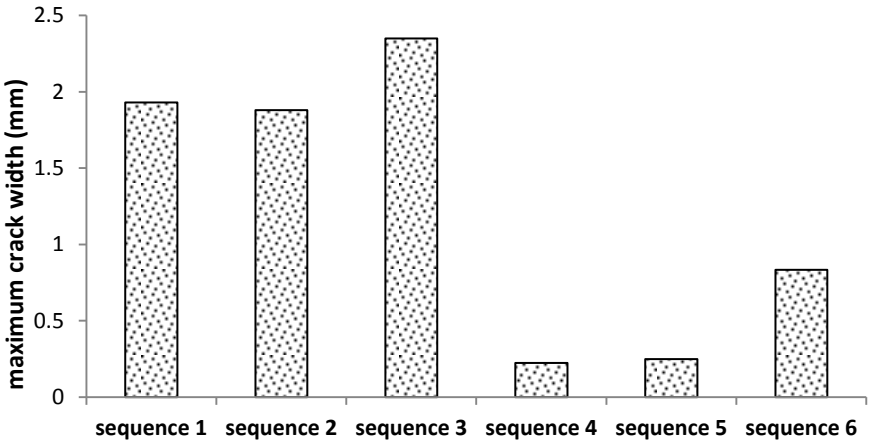

Figure 4.16: maximum damage for different excavation sequences

As mentioned earlier, the annular space has been assumed as the main source of volume loss in this study, and the gap between tunnel lining and excavation has not been forced to close during simulation of volume loss, but instead is limited to a value, required for attaining equilibrium. Figure 4.17 shows the displacement of crown, or invert (whichever is most) towards tunnel center line for each excavation stage (sequence 4), when tunneling simulation was done in a soil having elastic modulus of 35MPa. The maximum displacement of crown/invert was encountered for 5^{th} and 6^{th} excavation stages, and it was 10.5mm; the overcut in microtunneling operations, for a tunnel of 2m in diameter, is usually more than twice of that value.

Such high value of overcut is not suitable, as it can have significant effect on long term settlements, and is not required for an operation where steering of tunnels is not involved.

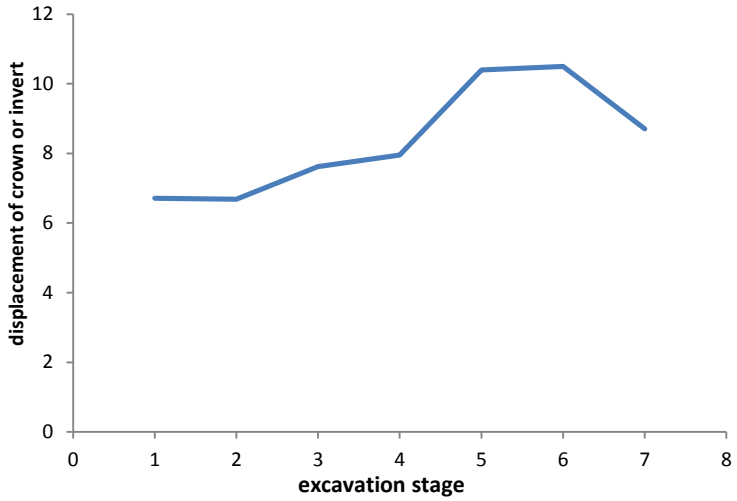

Figure 4.17: Closure of overcut in each excavation stage

4.2.2. Rough interface

The wall without openings sustained no damage for the case of rough interface. Four, as well as two, story wall was subjected to a closely-spaced microtunneling operation in soil having elastic modulus of 30MPa; mechanical properties of wall were assigned as MSN3.

The wall (4 as well as 2 story) with openings, all three opening configuration, sustained negligible/very slight damage -as defined by [17]- when subjected to simulation of closely-spaced microtunnels in soil having elastic modulus of 30MPa; mechanical properties of wall were assigned as MSN3, see earlier sections.

In the case of rough interface, concentration of stresses around corners of window openings was the source of maximum damage. The windows at edge of wall, at first story, were stressed most; window openings at upper levels were least effected, see Figure 4.20. The damage increased with excavation of tunnels, as curvature of wall lead to increased concentration at corners of openings, see Figure 4.21.

Rough interface has a beneficial effect on wall as it restricts relative movements between soil and ground in elastic regime, thus inducing compressive stresses in wall.

Figure 4.18 shows tangential interface stresses for three excavation stages. The interaction between soil and masonry increased as number of tunnels increased. Distribution of tangential and normal stresses, for 1st and 5th excavation stage (see Figure 4.18 and 4.19), indicate development of tilt in wall. Tilt also induces horizontal tensile stresses in wall.

The wall was analyzed against all six excavation sequences (see section 3.1).

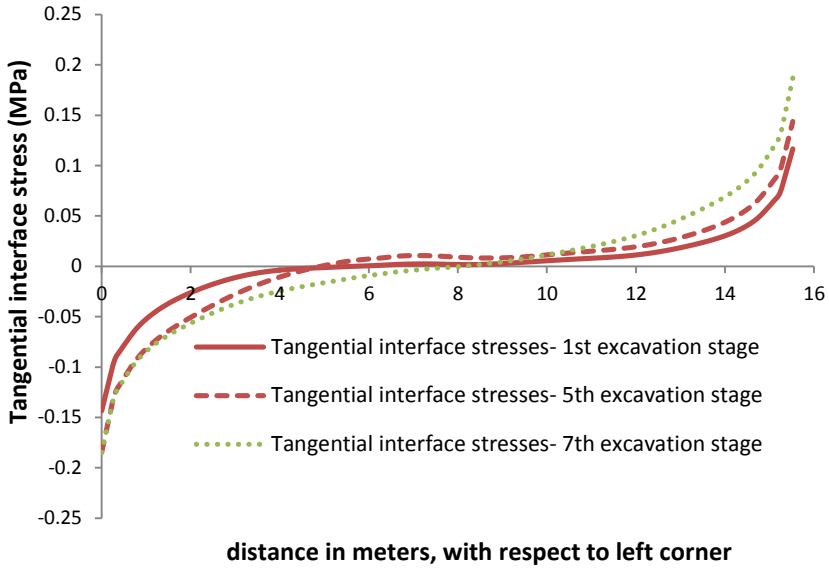

Figure 4.18: Tangential interface stresses, rough interface, and central-door

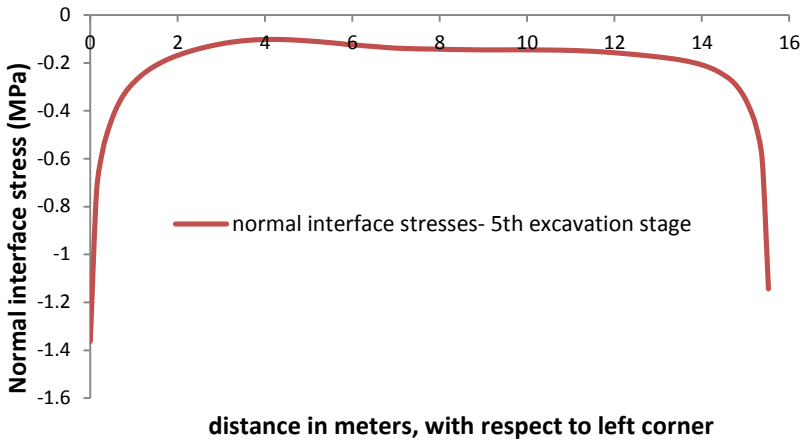

Figure 4.19: Normal interface stresses for 5th excavation stage indicates tilt in wall

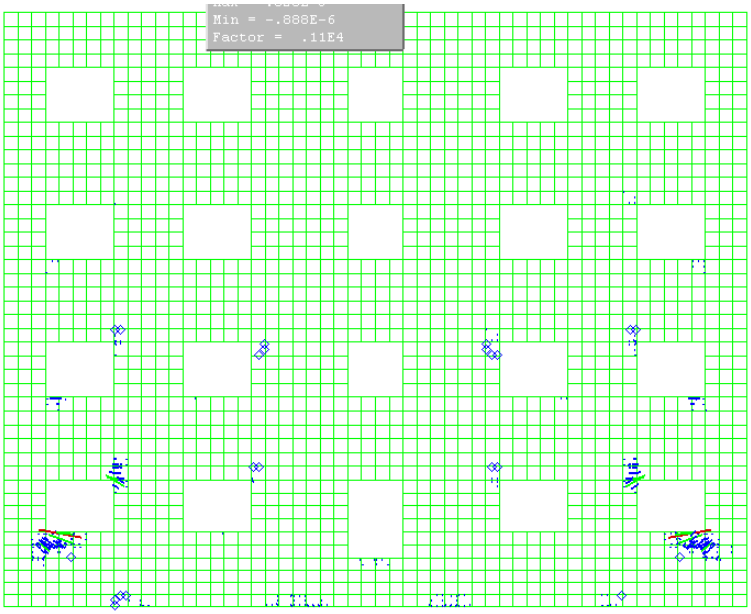

Figure 4.20: Concentration of damage around corners of openings

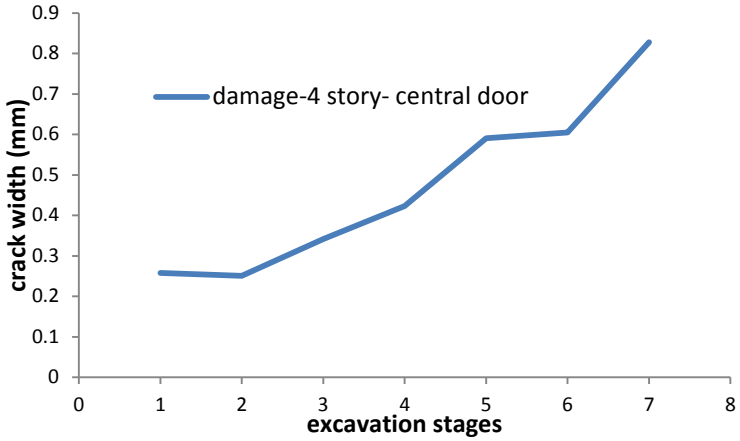

Figure 4.21: Increase in damage with excavation stages, central door

4.3. Wall isolated with 9-tunnel assembly

4.3.1. Smooth interface

For this wall, 'excavation sequence 1' (see section 3.1) induced least damage on wall for all opening configurations.

The Figure 4.22-4.24 shows the results that lead us to the conclusions, discussed in above sections: stiffer and stronger conditions of soil and masonry are required to keep the damage at particular level for heavier walls as compared to lighter walls (except wall without openings); the applicability of the innovative base isolation reduces as the length of building increases; walls having door openings are most susceptible to excavation work required for this innovative base-isolation technique; the wall with central door is expected to sustain most damage for a given set of conditions than other opening configurations; the wall, with window openings, performed much better; and the wall, without any openings, will sustain least damage.

For the wall without openings, 4-story wall sustained lesser damage than 2-story wall. Hence the increase in stiffness for 4-story wall due to height did outweigh the effect of increase in

loading, and the taller wall sustained lesser damage; this behaviour was not observed for previous two cases.

The Figure 4.23 highlights mechanical properties, required for a 4-story, so that the damage is limited to 1 mm crack; these properties are not representative of a historical construction. In actual situation, the shear resistance between interface of soil and foundation will not be negligible, which will lead to a lesser damage. Hence, the results, corresponding to smooth interface, represent upper bound of damage.

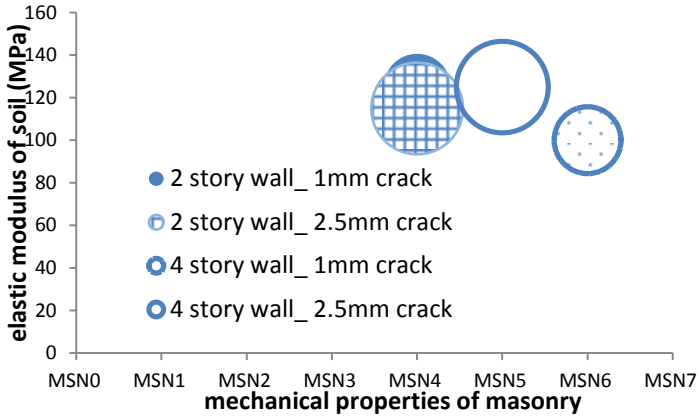

Figure 4.22: Mechanical properties of masonry and soil for different damage levels

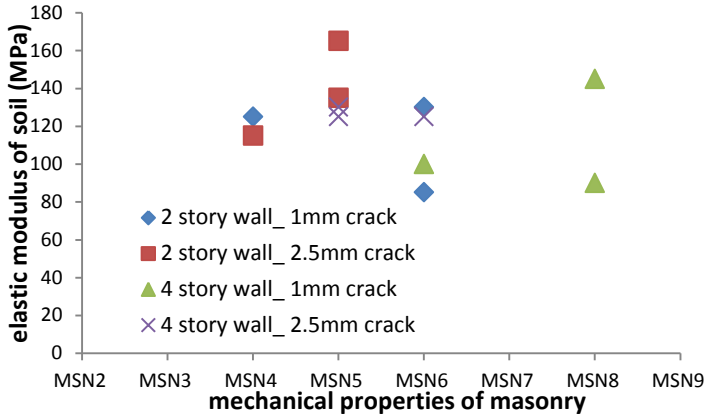

Figure 4.23: Mechanical properties of masonry and soil for different damage levels (scatter)

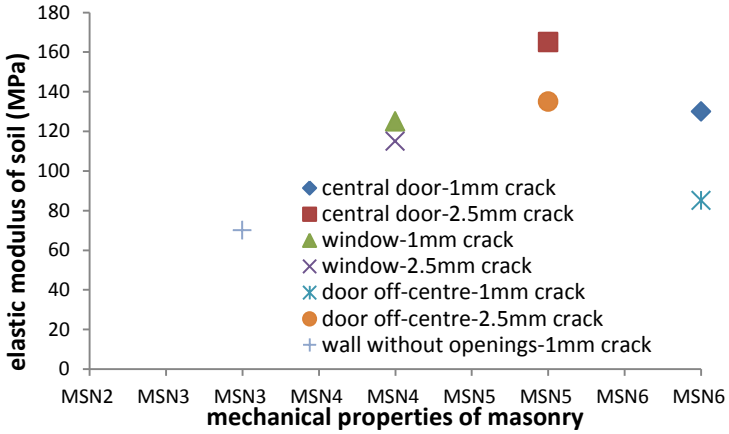

Figure 4.24: effect of opening configuration on damage susceptibility, 2 story wall

For a wall without opening, damage will lie in the bottom region of wall. Cracks will propagate in horizontal, as well as diagonal direction. Under the self-weight of wall, main stresses are tensile strains in horizontal direction (Figure 4.25), but as the tunneling process proceeds, diagonal strains became larger than horizontal strains. The first set of cracks to open will be in diagonal

direction; cracks will be distributed over a wider area for the case of wall without openings(Figure 4.26). Figure 4.25 shows crack distribution under the self-weight of wall; most stressed region lie in bottom center of wall, where maximum tensile stresses are the ones in in horizontal direction (area identified by an oval). Figure 4.26 shows crack distribution after excavation of all tunnels; cracks are distributed over much larger area, and maximum tensile stresses are in diagonal direction.

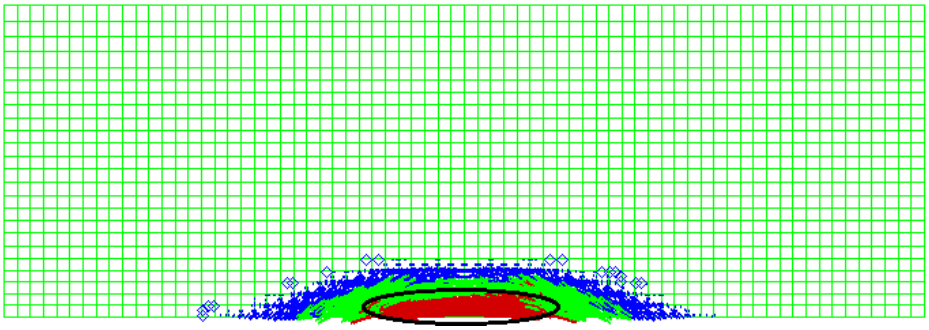

Figure 4.25: crack distribution under self-weight

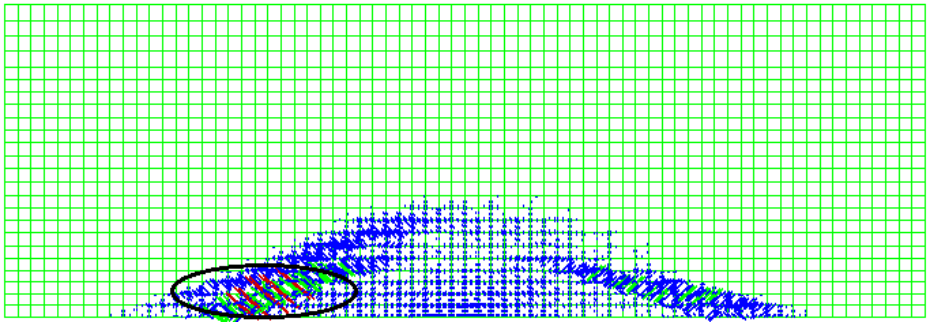

Figure 4.26: crack distribution after excavation of all tunnels

Figure 4.27 shows development of arching behaviour in the wall without openings. This arching behaviour leads to horizontal tensile stresses at bottom of masonry.

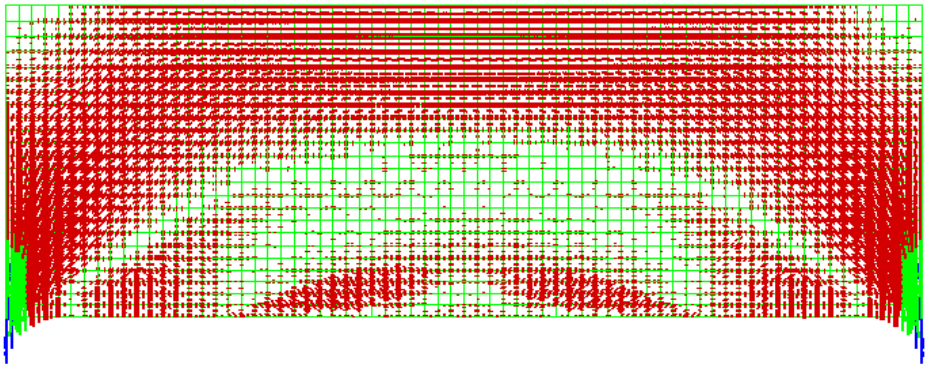

Figure 4.27: arching in wall with openings

As mentioned earlier in the section, 4-story wall (without opening) sustained lesser damage than 2 story for the same soil conditions, which is inconsistent with the results of previous two cases. Figure 4.28 shows the crack sustained by two walls at each excavation stage: in first four stages, weight of wall has a dominant effect, while bending behaviour is dominant for the next five excavation stages. Figure 4.29 shows deformed shape of 2-story after the completion of excavation of all tunnels, indicating that flexural behavior is dominant.

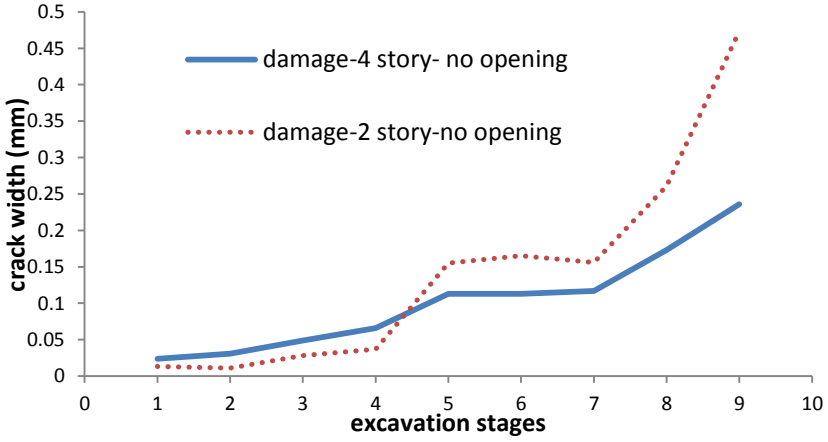

Figure 4.28: damage comparison for 2 and 4 story wall without openings

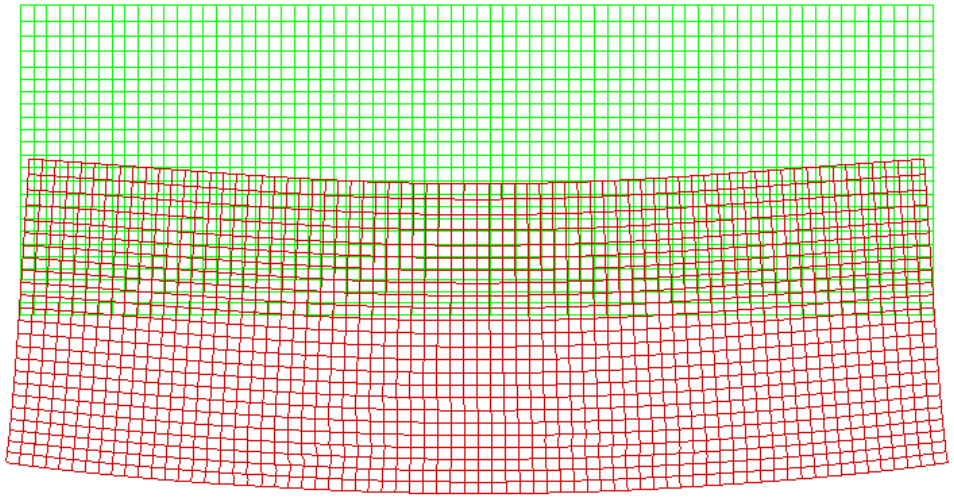

Figure 4.29: Deformed shape of two story wall, 9th excavation stage

The region around bottom of door opening was most stressed in tension for corresponding wall-configuration; In case of wall with window openings, maximum damaged zone was located at bottom center of wall. Damage was observed over larger area for a wall having openings for windows, while it spreaded over smaller area for a wall having openings for doors. The result highlights that the masonry wall with door openings is more susceptible to damage, related to vertical ground movements, than the wall without any opening for door. Figure 4.30-4.32 shows the crack distribution for three opening configuration, oval indicates maximum stressed area in tension.

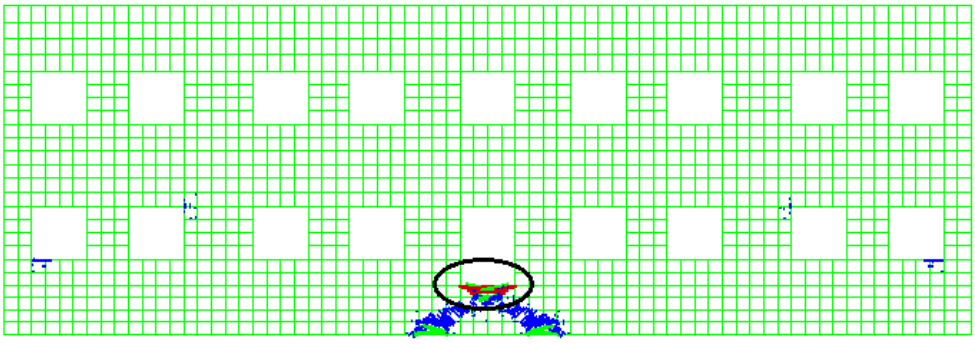

Figure 4.30: Distribution of cracks, central door

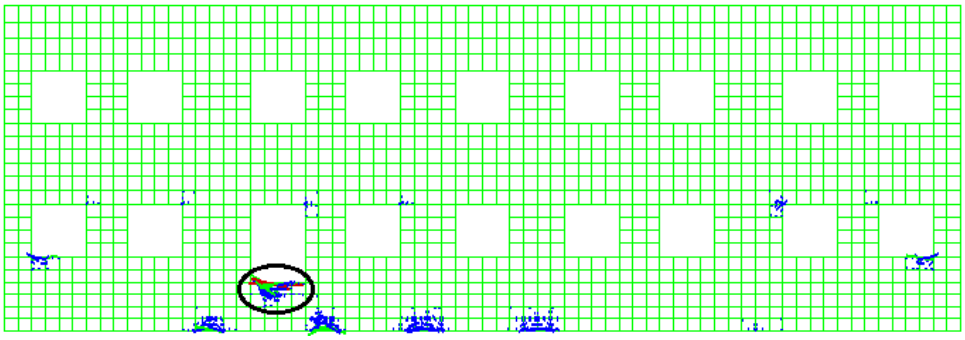

Figure 4.31: Distribution of cracks, off-center door

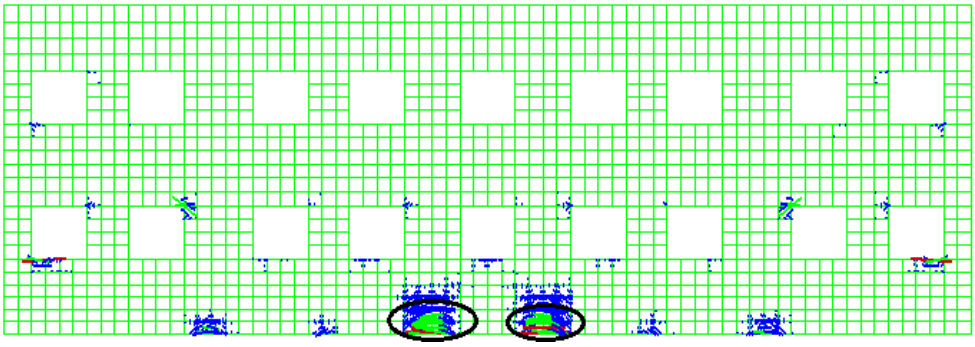

Figure 4.32: Distribution of cracks, window openings

Figure 4.33 demonstrates the importance of choosing appropriate sequence of excavation in limiting the damage related to the construction of closely spaced microtunnels. The results depicted in Figure 4.33 are for first 4 excavation sequences, see Figure 3.6. In sequence 3, excavation started from center, while other sequences commenced from outermost tunnel. Hence the sequence, in which excavation starts from ends, is much more favorable than the one in which excavation start from central region, and spreads towards ends.

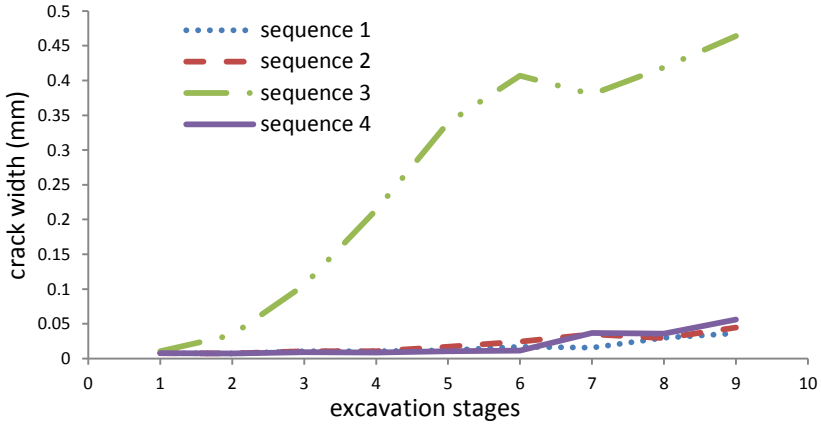

Figure 4.33: effect of excavation on damage susceptibility

Figure 4.34 and 4.35 shows distribution of interface stresses in normal direction at different stages of excavation for two types of wall. Normal stresses increased at the edges of wall, and consequently there was a reduction of stresses in the region in-between, as excavation process proceeded forward, indicating the redistribution of stresses due to the openings in soil medium. A small hump in the center of Figure 4.35 for different excavation stages indicates the concentration of vertical stresses around the door-opening, leading to additional differential movements and damage for that opening configuration.

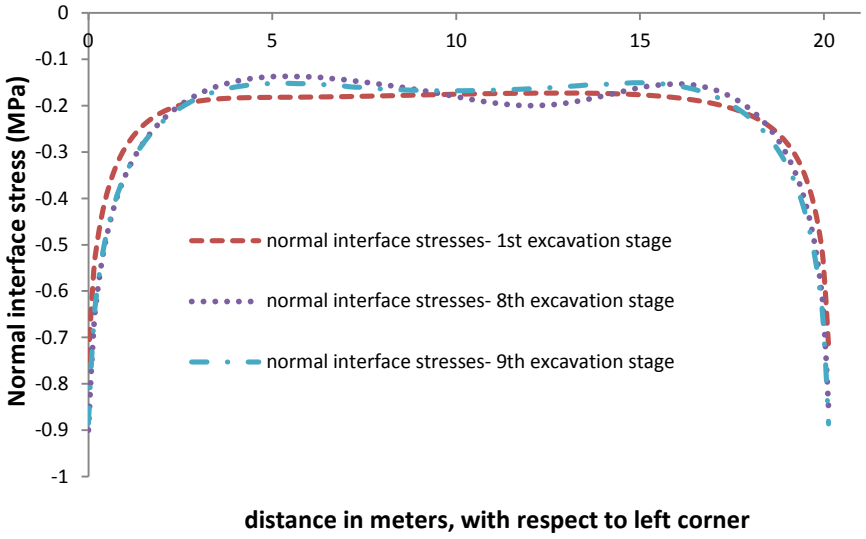

Figure 4.34: normal interface stresses for wall without opening

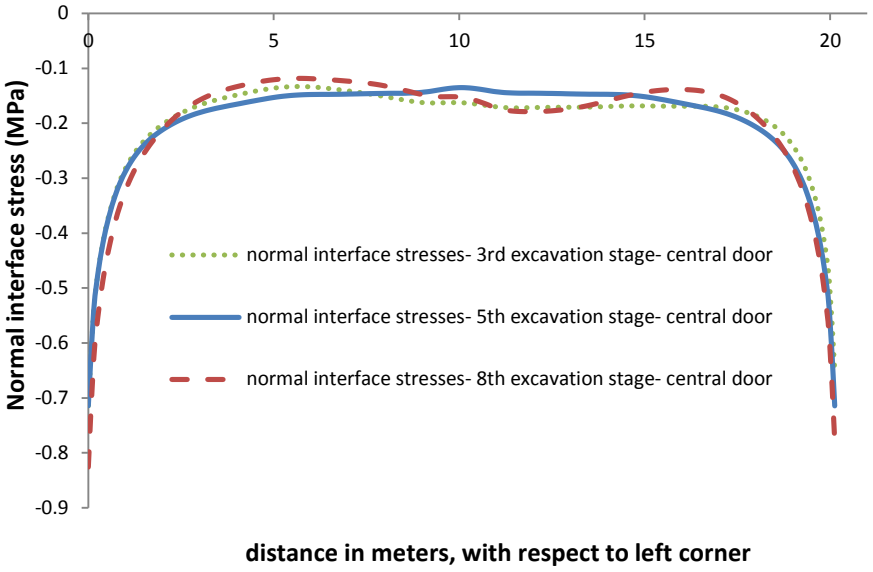

Figure 4.35 : normal interface stresses for wall having opening for door at center

4.3.2. Rough interface

Unlike the previous two cases (wall isolated with 6 and 7 tunnel assembly), two story wall without openings, did sustain damage in this case. Four story wall (without openings) did not sustain any damage when coupled with soil having elastic modulus of 30MPa and 80MPa soil (mechanical properties of masonry were assigned as MSN3). The damage, in the case of assembly of 9 tunnels, is attributed to the tensile stresses due to the multiple reversal of curvature, experienced by the wall during excavation simulation of tunnels. The stiffness of Wall in previous cases, 6 and 7 tunnel assembly, was enough to prevent damage due to reversal of curvature. The four story wall, in this case, was stiff enough to resist tensile stresses due to multiple reversal of curvature. The damage was accumulated in central region of wall. The damage was negligible-very slight [17], when two story wall(without opening) was coupled with soil having elastic modulus of 30Mpa (mechanical properties of masonry were assigned as MSN3); and the wall

sustained no damage when it was couple with soil having elastic modulus of 120MPa (mechanical properties of masonry were assigned as MSN3).

Figure 4.36 and 4.37 shows tangential interface stresses experienced by the wall at different excavation stages. Figure 4-37 shows a plot in different scale so as make the figure more lucid; the wall experienced curvature reversal for first, fourth and sixth excavation stage. Figure 4.38 shows distribution of cracks for 2 story wall without opening.

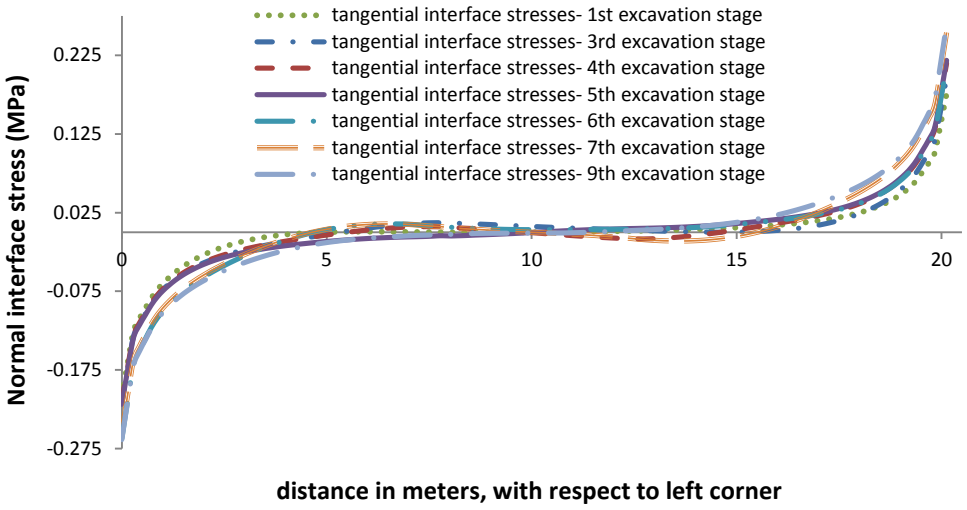

Figure 4.36: tangential interface stresses, wall without opening

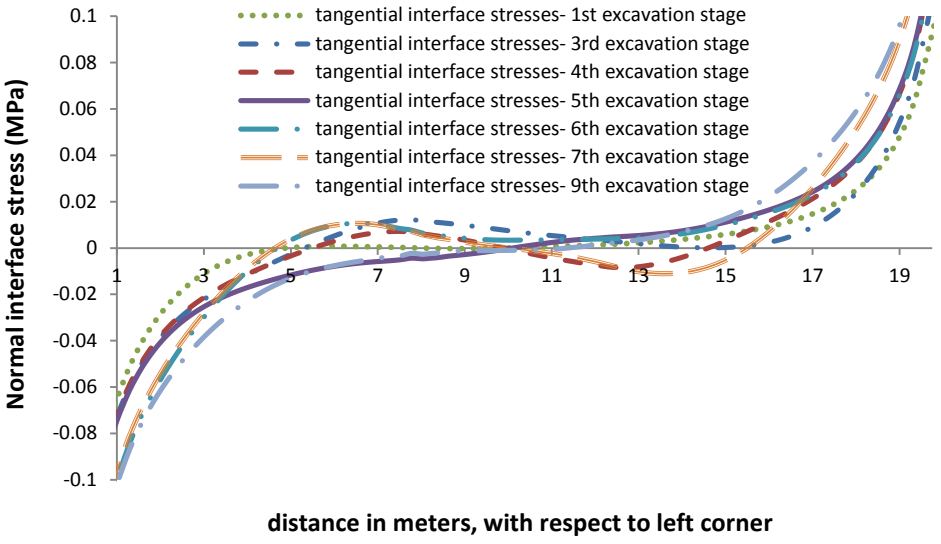

Figure 4.37: tangential interface stresses, wall without opening, zoomed

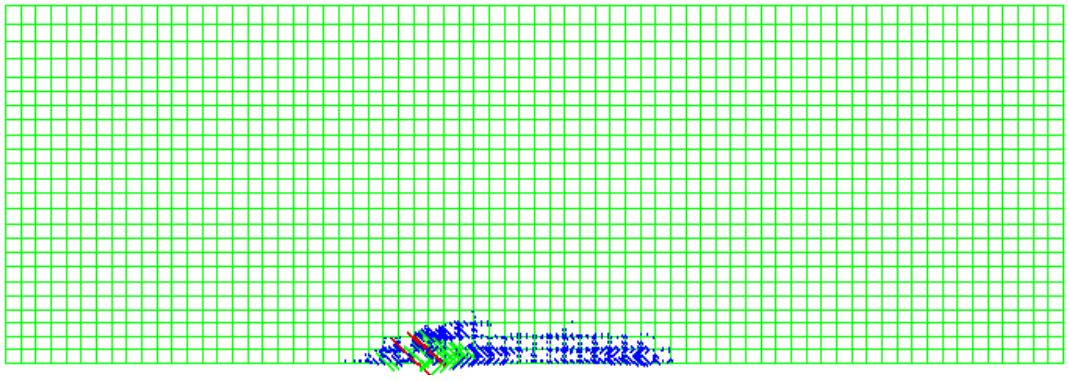

Figure 4.38: Distribution of cracks in two story wall without opening

The two story wall, with openings for door or windows or both, sustained negligible-very slight damage (maximum crack width 0.1-0.5mm), while 4 story wall sustained very-slight

(maximum crack width of about 1mm) damage when coupled with soil having elastic modulus of 30MPa; all walls were assigned mechanical properties corresponding to MSN3. All types of walls sustained similar damage when they were coupled with soil having elastic modulus of 130MPa, showing that the stiffness of soil has a negligible effect, which is unlike the behavior, observed in the case of smooth interface. Maximum damaged area was located at the corners of windows located at the edges of wall on first story. The bottom central area of wall also sustained damage due reversal of curvature. Taking overall picture, damage increased as the number of tunnels, excavated under wall, increase. Having said that, damage can stay at the same level for two consecutive excavation stages, which will depend on the excavation sequence, see Figure 4.41. Figure 4.39 and 4.40 shows distribution of cracks after the completion of all excavation of all tunnels. Figure 4.41 shows evolution of damage with excavation stages.

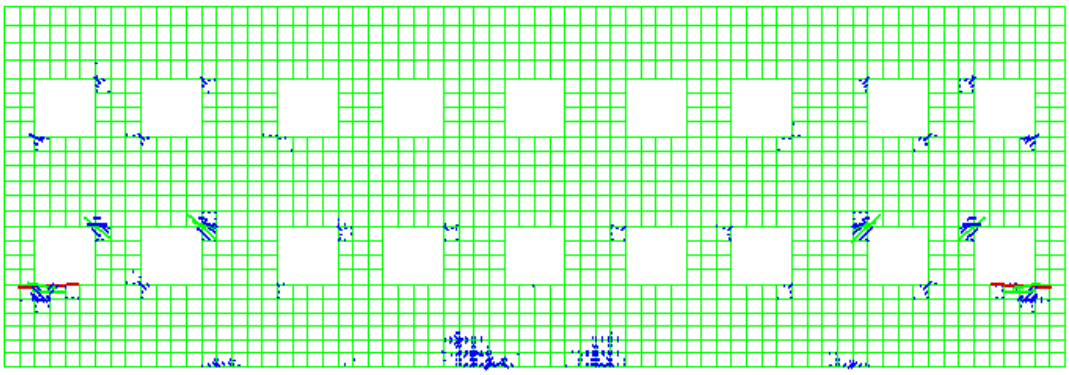

Figure 4.39: Distribution of cracks, window opening

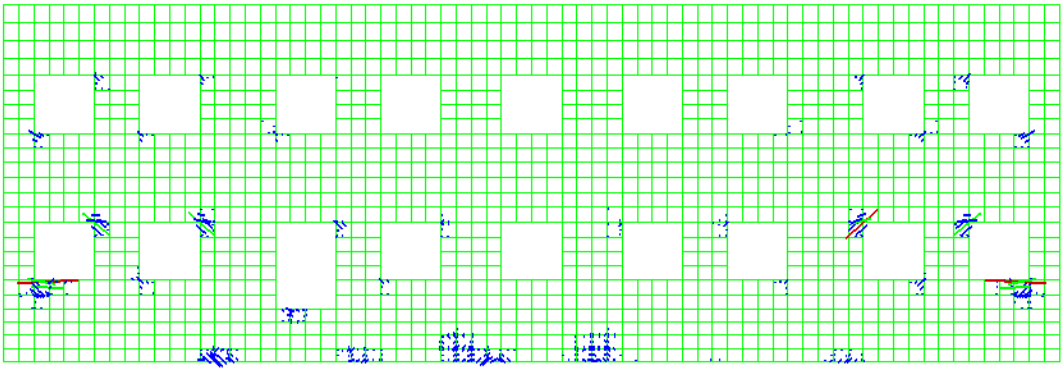

Figure 4.40: Distribution of cracks, door off-center

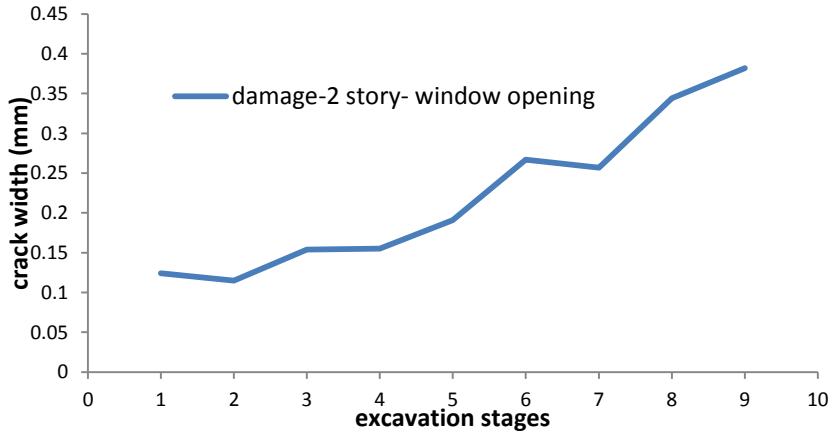

Figure 4.41: damage at each excavation stage for 2 story wall with window opening

4.4. Wall isolated with assembly of 10 tunnels

4.4.1. Smooth interface

Different excavation sequences were investigated for each type of wall, as stated in section 3.1, and, among them, 'excavation sequence 1' induced least damage on wall.

Figure 4.42-4.44 shows the results that show the continuation of a trend, observed in earlier results: damage susceptibility of wall will increase as length of the wall, perpendicular to tunneling process, will increase; presence of openings will have detrimental effect on wall, and the wall without openings will behave in much more favorable manner than the wall with openings; wall, with only window openings, are less susceptible to damage than the wall having openings for door; the wall, supporting a door at central region, is expected to sustain most damage for a given set of conditions than other opening configurations; stiffer and stronger conditions of soil and masonry are required to keep the damage at particular level for heavier walls as compared to lighter walls (except wall without openings).

In this case, as was seen in previous case of 9-tunnel-assembly, wall, without openings, behaved differently: taller wall sustained lesser damage than shorter wall. Hence the increase in axial stiffness for taller outweighed the increase in horizontal tensile strains due to weight of wall and the wall sustained lesser damage; this behaviour was not observed for previous first two cases (6 and 7-tunnel-assembly), and the wall, with openings, also did not exhibit the same behavior.

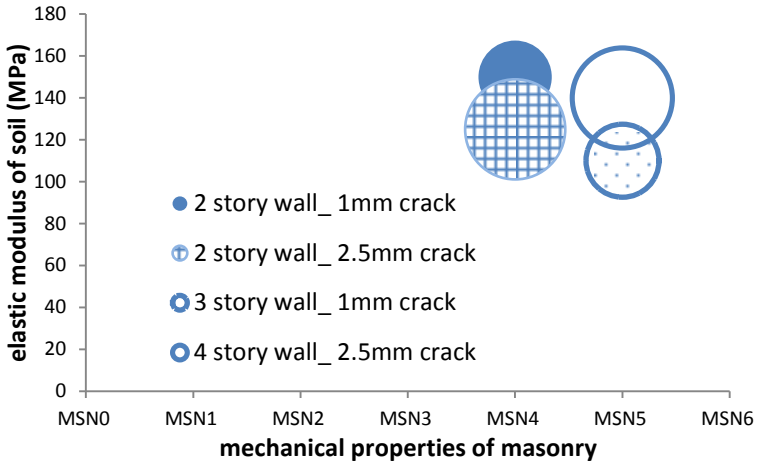

Figure 4.42: Mechanical properties of masonry and soil for different damage levels

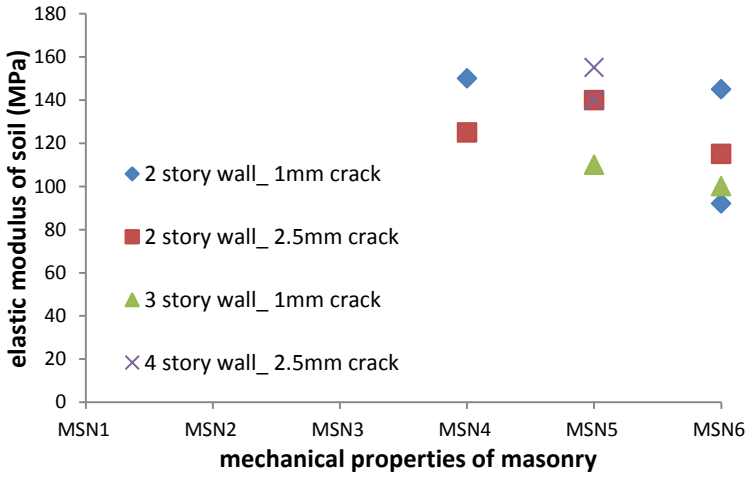

Figure 4.43: Mechanical properties of masonry and soil for different damage levels (scatter)

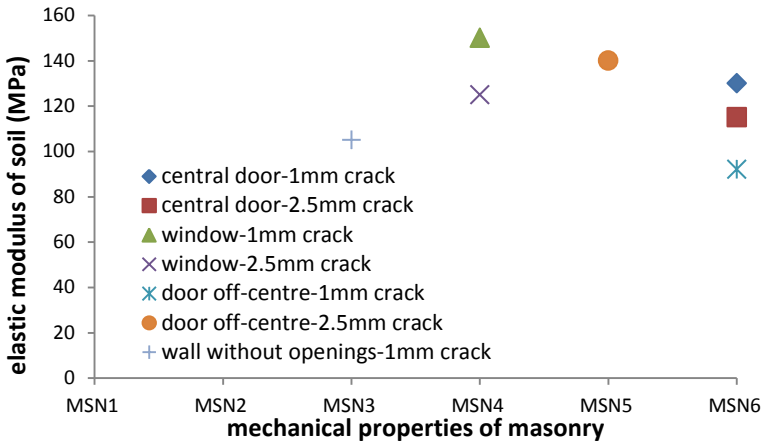

Figure 4.44: effect of opening configuration on damage susceptibility, 2 story wall

As discussed earlier, concentration of stresses around door opening lead to much more differential movements in vertical direction, over a short distance, than other opening configurations, which lead to more damage than other opening configurations. Figure 4.45-4.47 shows the curvature of wall, for three opening configurations, after the completion of eight excavations; three results were taken against same mechanical properties of soil and masonry. It can be seen that the curvature of wall without openings is smooth, while curvature of wall with door opening is very abrupt in central region. The curvature of wall with only window-openings has very little local disruptions.

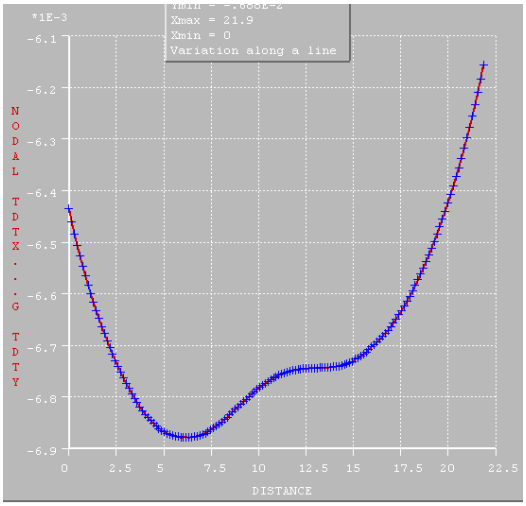

Figure 4.45: bending curvature of wall without openings

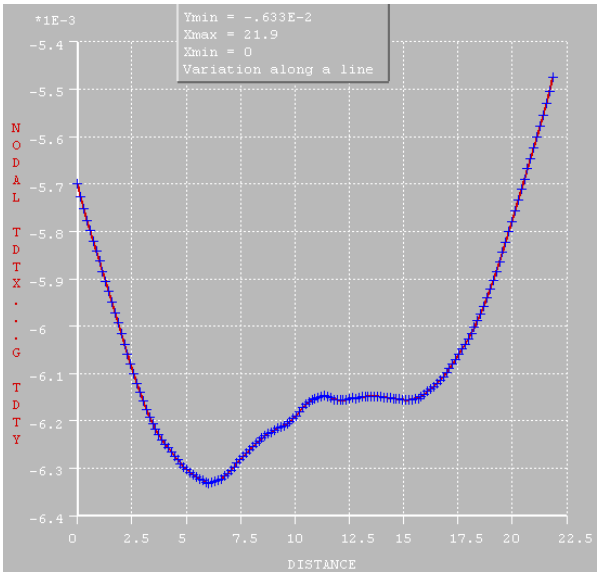

Figure 4.46: bending curvature of wall with window-openings

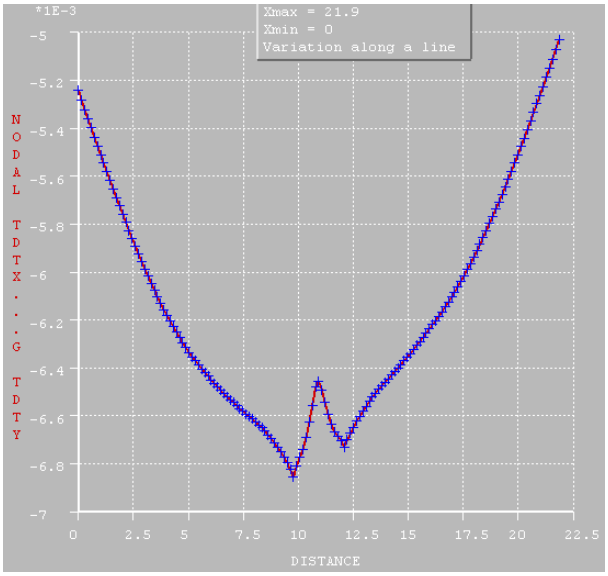

Figure 4.47: bending curvature of wall having door at center

Figures 4.47a, 4.48-4.50 show distribution of cracks for three opening configurations, after the excavation simulation of all tunnels. For wall, without openings, damage is scattered over much wider area than walls supporting openings for doors and windows. Presence of door opening has resulted in constriction of damage around door (Figure 4.49-4.50). Overall behavior that can be observed from the results of Figure 4.47a, 4.48-4.50 is that the presence of opening for door, in the center of wall, will result in constriction of damage in very narrow area, while the damage will spread over larger area in case of wall supporting only window-openings.

In Figure 4.47a, 4.48-4.50, region highlighted by oval, is the one that is affected most by tensile stresses. For walls, supporting openings for doors and windows, cracks initiated by horizontal tensile stresses at the interface, or at the bottom of door openings, while for wall, without openings, cracks (one's having maximum width) are initiated by diagonal tensile stresses. Hence, door openings will attract maximum damage. No damage has been observed on top of walls, indicating that hogging behavior is not critical for this type of tunneling process.

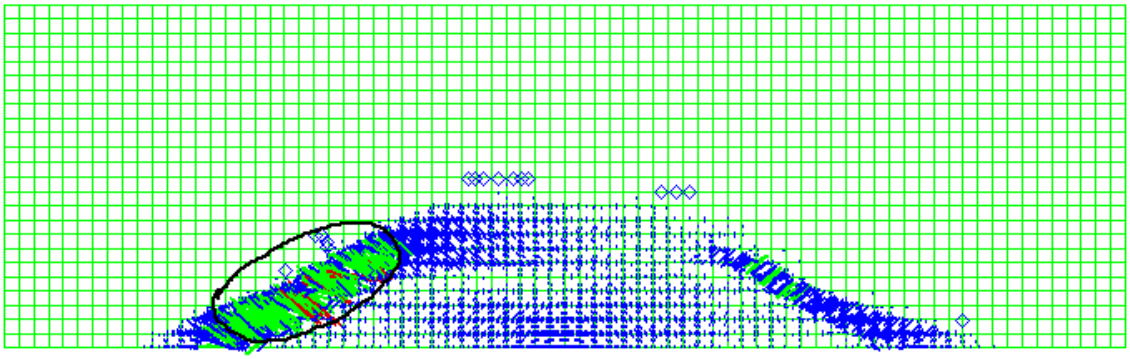

Figure 4.47a: Crack distribution of wall without openings

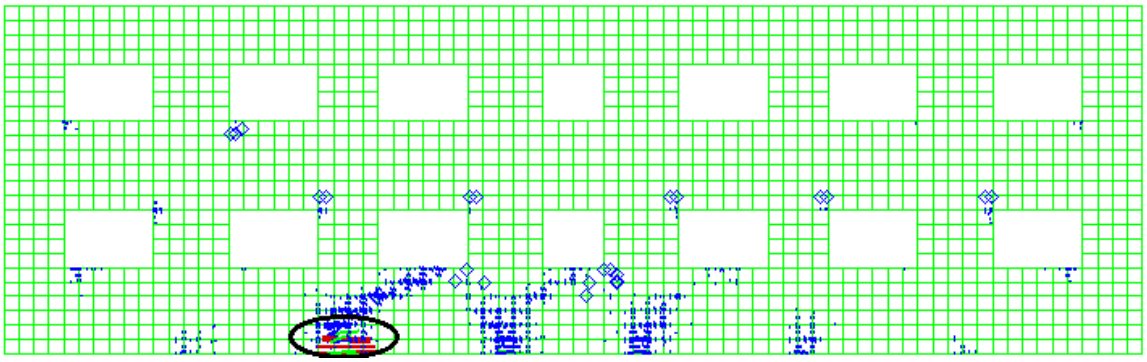

Figure 4.48: Crack distribution for wall with window-openings

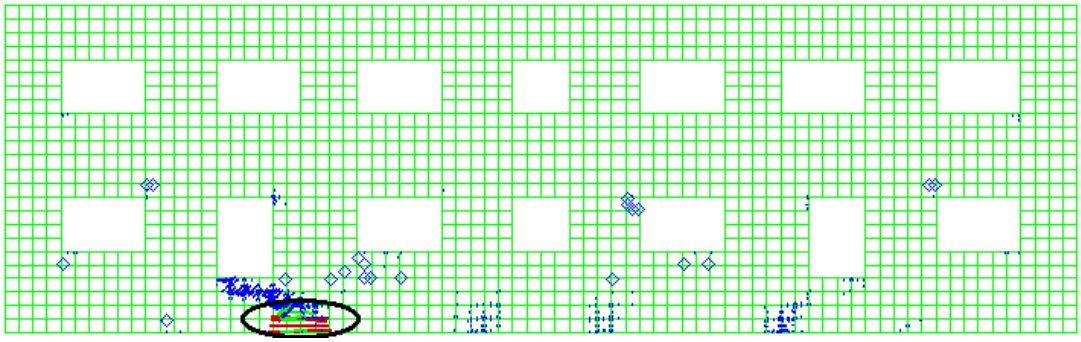

Figure 4.49: Crack distribution for wall having off-center door location

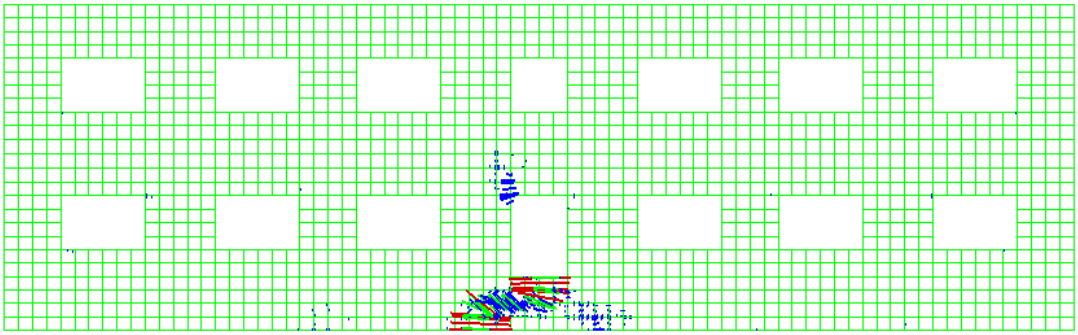

Figure 4.50: Crack distribution for wall with door located in central region

Walls, which will require odd number of tunnels, will experience a permanent tilt after excavation of all tunnels, as it is not possible to adjust excavation sequence that will induce symmetric settlements. Amount of tilt will depend upon the mechanical properties of soil. Wall, requiring even number of tunnels, will not experience tilt, unless, there is a situation of soil exhibiting plastic behavior. Figure 4.51 and 4.52 compares the curvature of wall for two cases: 10 and 9 tunnel assembly. However, maximum value of tilt, encountered in this study, was less than 0.2mm/m, which will not be noticeable [31].

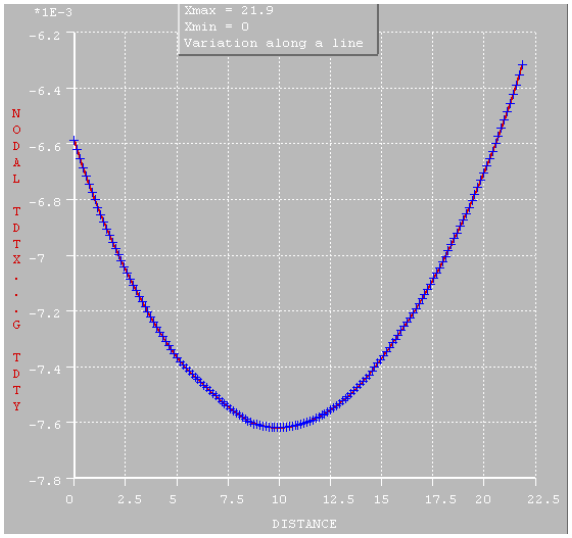

Figure 4.51: curvature of wall, showing tilt after completion of 10 excavations

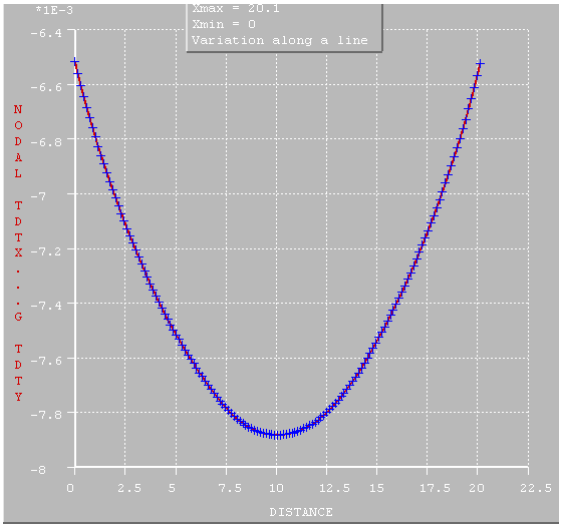

Figure 4.52: curvature of wall, showing no tilt after completion of 9 excavations

Figure 4.53 and Figure 4.54 shows effect of excavation sequence on damage susceptibility of masonry wall to construction of closely spaced microtunnels. These results are shown for eighth excavation stage. The figure shows importance of selecting appropriate excavation sequence for the application of this method; inappropriate excavation sequence can lead to a damage that can be much more, or even prove to be destructive, as compared to an appropriate excavation sequence.

The results also show that the excavation sequence, for which tunneling proceeds from inside to outwards, is much more destructive than the one for which tunneling proceeds from outwards to inwards. Appropriate sequence seems to be the one that starts from two outermost tunnels. The results in Figure 4.53-4.54 have been divided into two parts to make them lucid.

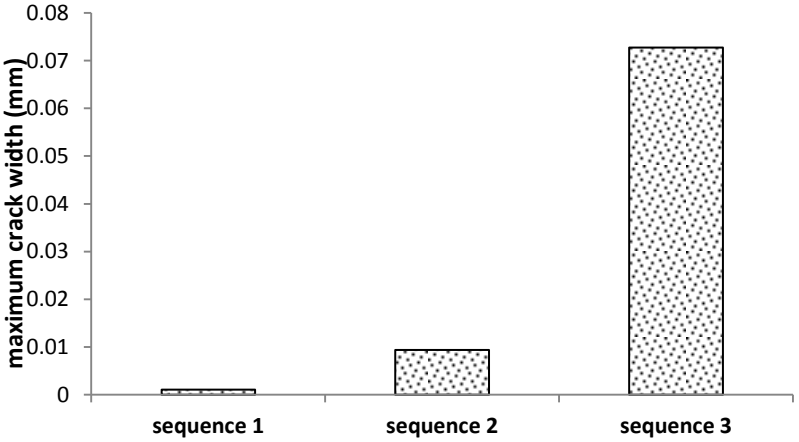

Figure 4.53: Effect of excavation sequence on damage susceptibility

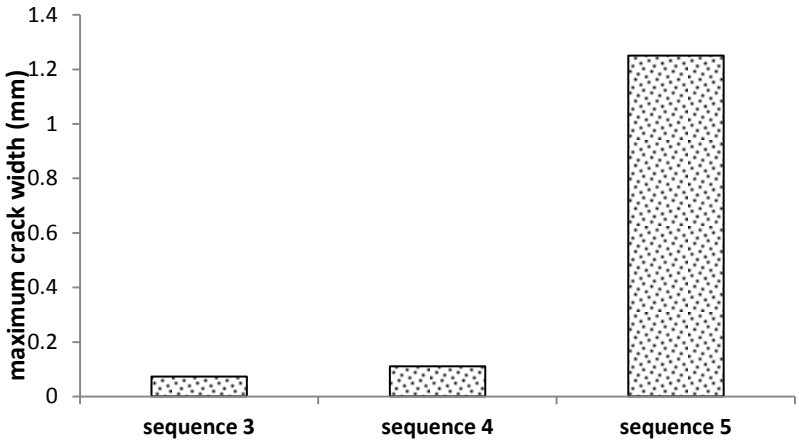

Figure 4.54: Effect of excavation sequence on damage susceptibility

4.4.2. Rough interface

The two story wall, without openings, sustained negligible-very slight damage, in this case as well, when subjected to tunneling in soil having elastic modulus of 35MPa; the wall sustained no damage for soil having elastic modulus of 135MPa. In addition to multiple reversal of curvature, as discussed in previous section, cracks also appeared due to horizontal tensile strains , developed before start of excavation process; these tensile strains develop due to soil structure interaction under self-weight of wall, before the start of excavation process. Figure 4.55 shows development of damage during excavation of tunnels; '0' refers to damage under self-weight of wall, before start of excavation process.

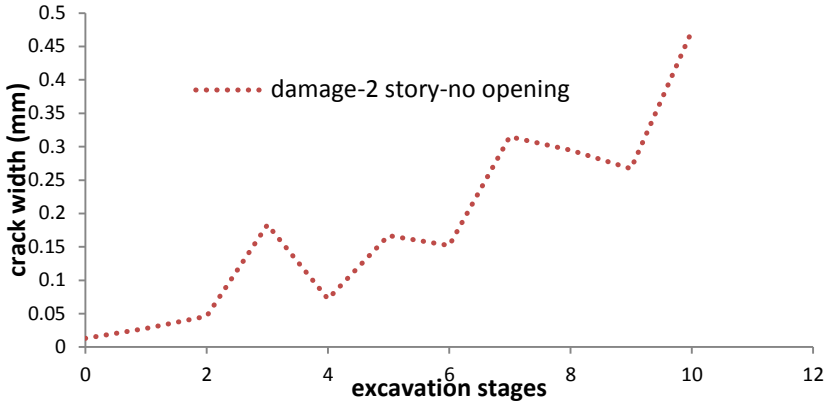

Figure 4.55: damage with respect to excavation stages, 2 story wall, rough interface

Four-story wall without openings, sustained no damage when it was subjected to tunneling in soil having elastic modulus of 35MPa. These results are in contrast to the results of 6 and 7-tunnel assembly, where taller wall experienced more damage than shorter wall.

Wall with openings behaved differently than the previous cases, where wall, with openings, sustained maximum damage around window openings.

In case of wall with opening for central door, concentration of stress around door opening induced diagonal tensile stresses below the door, which lead maximum damage around door opening. Two story wall sustained more damage than the four story wall. Four-story wall sustained maximum damage around window opening. Figure 4.56 and Figure 4.57 show distribution of cracks for 2 and 3 story wall, with opening for door at central area. In these figures, Oval shows location of maximum damage. Figure 4.58 compares damage between 2 story and 3 story wall, having door at central area. Result show that the increase in stiffness of wall, due to its height, can reduce damage susceptibly of wall, thus overcoming the effect of increase in weight.

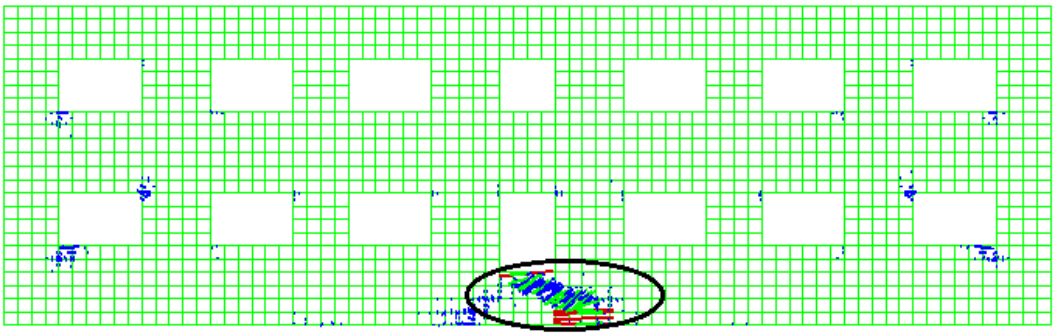

Figure 4.56: Distribution of cracks for 2 story wall

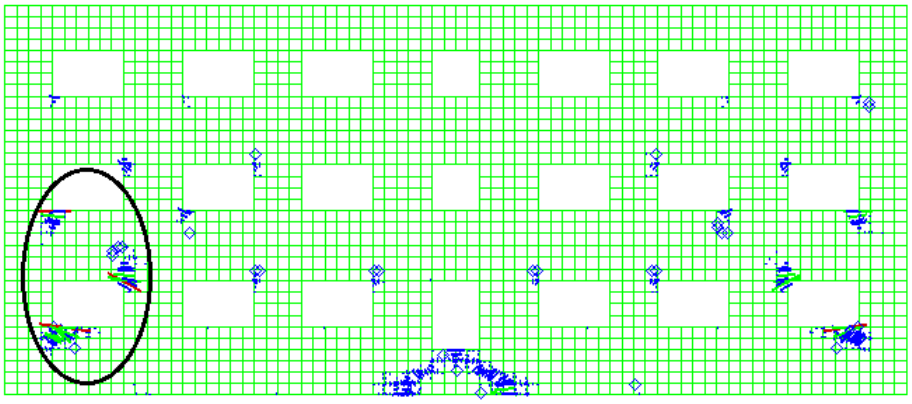

Figure 4.57: Distribution of cracks for 3 story wall

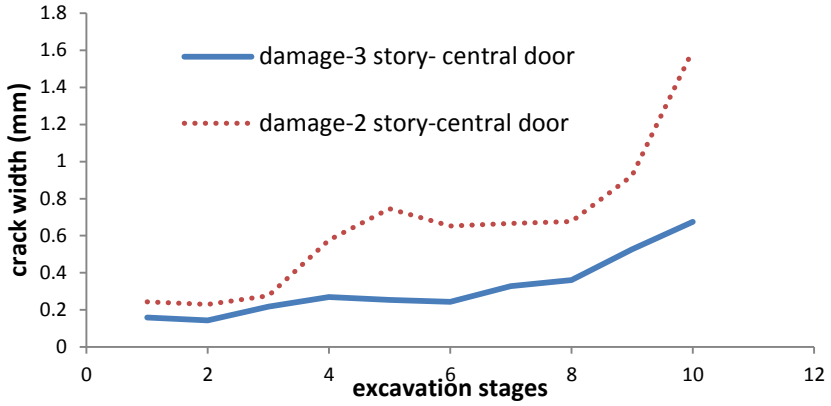

Figure 4.58: damage with respect to excavation stages, 2 and 3 story wall, and rough interface

In the case of walls, having window and off-center door, location of maximum damage was around window opening at almost all excavation stages. Maximum damage sustained by these walls was less than the wall having central-door. Figure 4.59 compares damage sustained by all three opening configurations, as well as damage sustained by wall without openings. Results are shown for 2 story wall, subjected to tunneling in soil having elastic modulus of 35MPa. Wall, having door at central region, sustained maximum damage, while all other cases sustained a similar amount of damage.

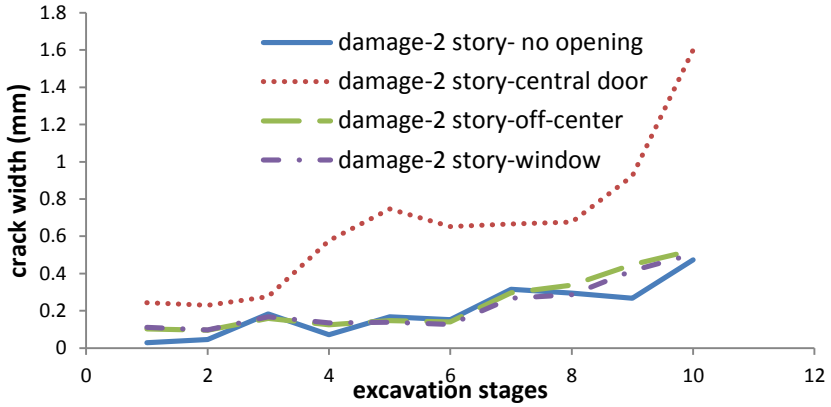

Figure 4.59: Comparison of damage for wall of different configurations

4.5. Chart: summary of some results

Figure 4.59b shows summary of some of the results of study. The chart has been plotted in terms of non-dimensional values. X axis of chart contains length to height ratio of walls, while entries of Y axis have been plotted in terms of a non-dimensional parameter, which is representative of the strength and stiffness of soil and masonry. The parameter has been computed as the ratio of product of various strength and stiffness values, used in the study for masonry and soil, to a product of base values of strength and stiffness values of soil and masonry. Strength and stiffness values used for that non-dimensional parameter are E_m, F_t, G_f and E. Hence, larger value of that non-dimensional parameter, along y-axis, represents stronger and stiffer condition of soil and masonry.

Figure 4.59b shows the mechanical properties required for soil and masonry, for different values of length to height ratio, and for a wall of particular opening configuration, so that damage is limited to a particular level (maximum crack width of about 2.5mm). The chart has been divided into two story and 4 story entries, and also in terms of opening configuration.

The figure 4.59b shows the effect of opening configuration of wall on its damage susceptibility. Stronger and stiffer conditions of soil and masonry are required, for a wall of particular length to height ratio, to limit damage to particular level for a wall having door-opening at central region than other types of wall. Wall, with particular length to height ratio, and supporting door-opening at central region, will sustain more damage than other opening configurations for a given condition of soil and masonry; wall without openings will sustain least damage in similar scenario.

The figure also shows effect of self-weight and applied loads on susceptibility of wall to damage.

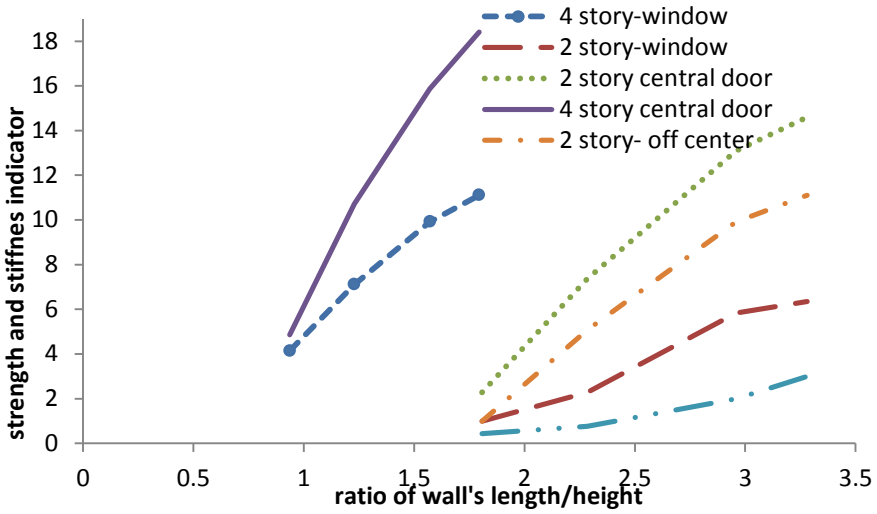

Figure 4.59b: effect of opening configuration and applied loads

4.6. Effect of depth of tunnel assembly

Effect of depth of tunnel assembly was investigated by considering four depths: 5, 6, 7 and 8m. Two-story wall, without openings, was analyzed for that purpose. Figure 4.60-4.62 shows maximum damage experienced by three different walls under different depths of tunnel assembly.

The result show that the two story wall, requiring 6 tunnels, is not susceptible to different depths of tunnel assembly, considered in this study.

Two-story wall, requiring 7 and 9 tunnels, is susceptible to depth of tunnel assembly. In these cases, wall subjected to tunnel depth of 8m sustained much more damage than tunnel depth of 5, 6 and 7 meter. Walls sustained almost same damage for tunnels-depths of 5, 6 and 7 meter.

These results show that behavior wall with depth is dependent on its L/H ratio.

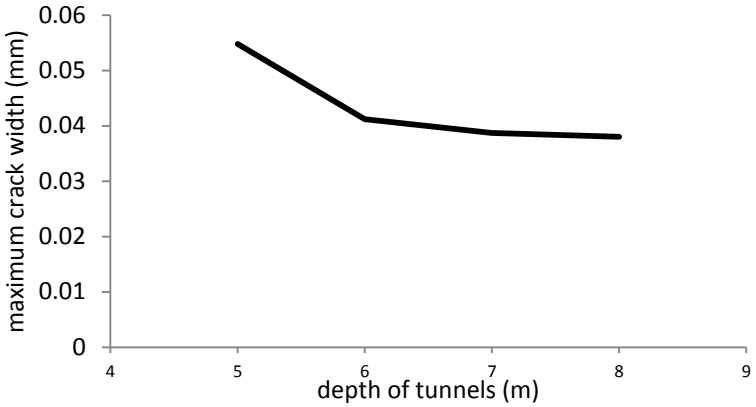

Figure 4.60: Behaviour of wall with depth, wall over 6-tunnel assembly

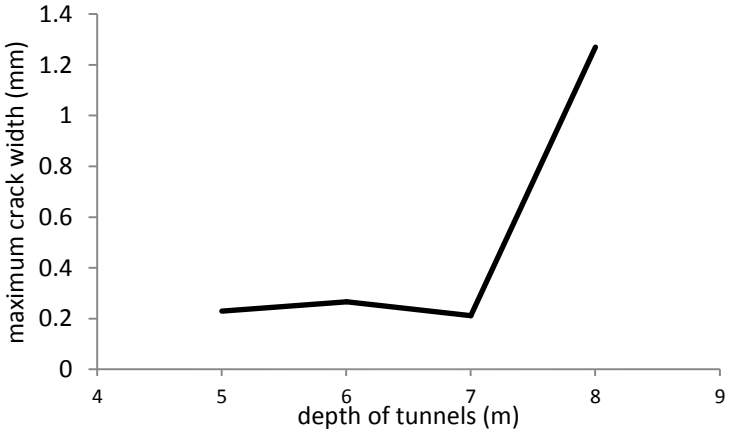

Figure 4.61: Behaviour of wall with depth, wall over 7-tunnel assembly

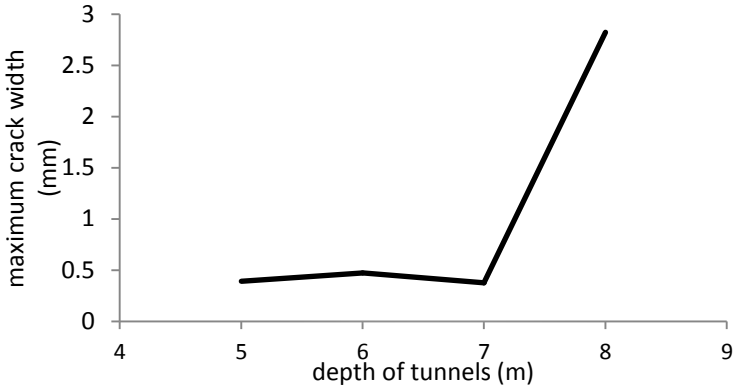

Figure 4.62: Behaviour of wall with depth, wall over 9-tunnel assembly

4.7. Effect of normal stiffness of interface

As discussed earlier, tangential stiffness of interface affects the damage sustained by masonry during excavation of tunnels. Having said that, normal stiffness also affects the damage susceptibility of masonry [32]. Figure 4.63 compares the damage sustained by masonry wall during tunnelling process for three values of normal stiffness of interface; masonry sustained maximum damage for the k_n value of 8E +8. Higher values of normal stiffness resulted in highly nonlinear distribution of normal interface stresses in the middle region of wall which increased relative vertical displacements and, hence, induced more damage.

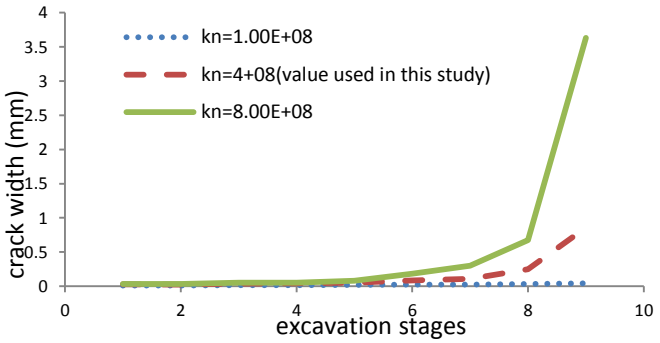

Figure 4.63: effect of normal stiffness of interface elements

4.8. Damage indicators

Monitoring is one of the important part of tunnel construction, which can give warning for expected level of damage, important field data, and it can help in validating, or improving, mathematical model. Monitoring of building damage during construction process will depend on reliable damage indicator. Different damage indicators have been proposed in the past as discussed in section 2.4.

This section will present results of a study [33], in which relationship of different indicators was investigated with damage; damage was defined in terms of maximum crack width and mean crack width. The damage indicators, investigated in that study are: deflection ratio(DR); angular distortion(β); average horizontal strain(ε_h), defined as the maximum change in length of wall at the foundation level over a distance of 1m; maximum change of slope ($\Delta\theta$); tilt; and maximum differential settlement.

Walls requiring 6, 7 and 11 tunnels were analyzed in that study. One type of opening configuration, door located at center, for walls requiring 6 and 7 tunnels, while two types of opening configurations (central door and off-center door) were considered for wall over assembly of 11-tunnels.

Different mechanical properties of soil and masonry were used for this section, section:4.8, and they are not mentioned here, as the objective, here, is to show relationship between different damage indicators and damage sustained by masonry over different excavation stages during simulation of tunneling process.

Only excavation sequence 1(Figure 3.4) is considered for assembly of 6 tunnels, first three excavation sequences (Figure 3.5) are considered for assembly of 7 tunnels. Figure 4.106 shows opening configurations considered for 11-tunnel assembly.

Figure 4.64-4.69 shows evolution of damage and damage-indictors with excavation stages for wall over 6-tunnel assembly; each data point corresponds to an excavation stage, and shows value of damage-indicator at that particular excavation stage. In these figures, values of β and DR are zero in the first excavation stage. Hence, the damage experienced by the masonry is due to the soil subsidence under the self-weight and superimposed load. The first excavation resulted in tilt and the second excavation eliminated the tilt produced due to first excavation. Hence the tunnel-related damage started during the third excavation. Tilt is a result of adopted excavation sequence, as excavation started from the outermost tunnels (see Figure 3.4). In the light of these results, ε_h provided the best correlation with damage, while DR and $\Delta\theta$ provided a poor correlation.

In Figures 4.64-4.69, 'crack max' refers to maximum crack width; 'crack mean' refers to mean width of all cracks.

Figure 4.70-4.81 shows evolution of damage and damage-indicators with excavation stages for wall over 7-tunnel assembly; each data point corresponds to an excavation stage, and shows value of damage-indicator at that particular excavation stage. Three different excavation sequences were considered in this case. Tunnel-related damage started during in the third excavation, as in the case of 6-tunnel assembly, for sequences 1 and 2, while it started from the first excavation for sequence 3.

The excavation sequence appears not only to play a vital role in the evolution of damage with excavation stages but also influences the total damage experienced by the masonry wall. Damage increased considerably in the last two excavation stages, and the wall experienced much more damage in the case of sequence 3 than in the other sequences; sequence 2 inflicted least damage.

Assuming sequence 2 is chosen in design, ε_h provides again the best correlation with damage; β provides the second best.

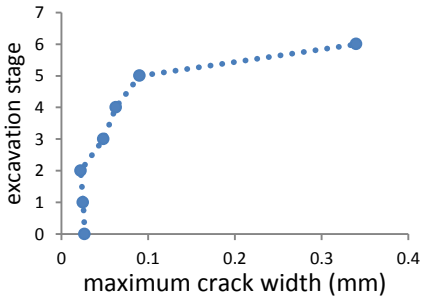

Figure 4.64: Crack max evolution

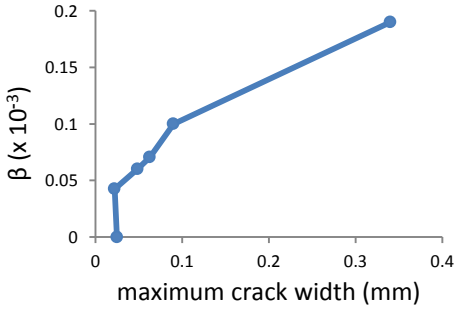

Figure 4.65: β vs. crack max

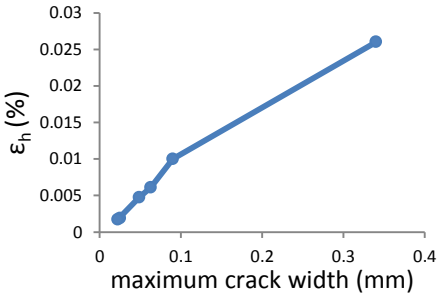

Figure 4.66: εh vs. crack max

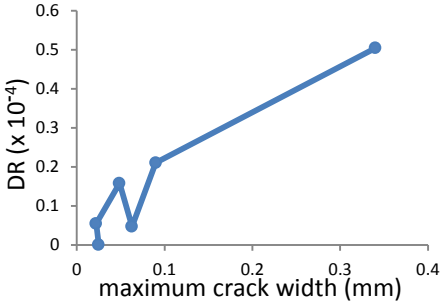

Figure 4.67: DR vs. crack max

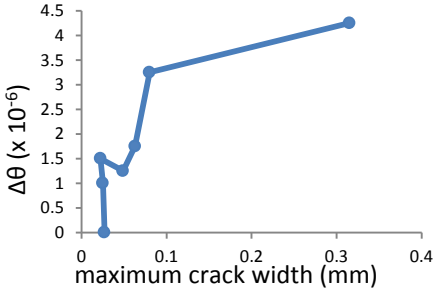

Figure 4.68: Δθ vs. crack max

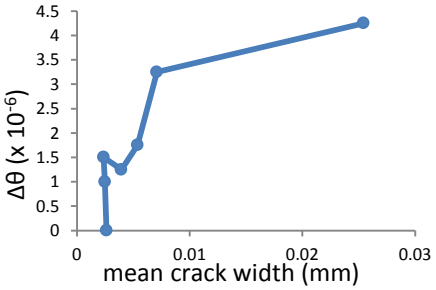

Figure 4.69: Δθ vs. crack mean

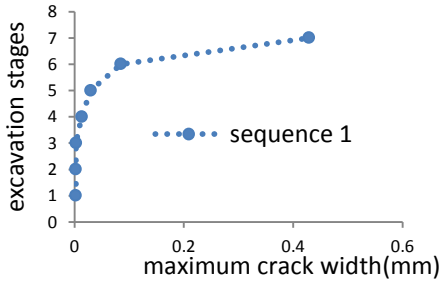

Figure 4.70: Crack max evolution

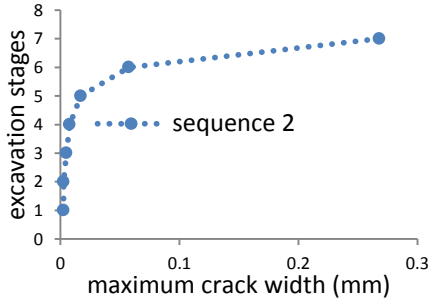

Figure 4.71: Crack max evolution

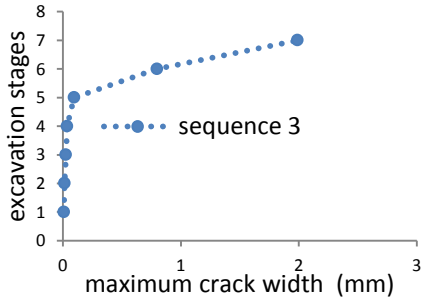

Figure 4.72: Crack max evolution

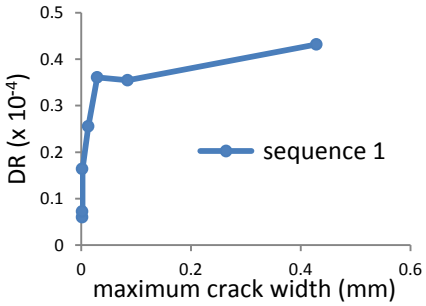

Figure 4.73: DR vs. crack max

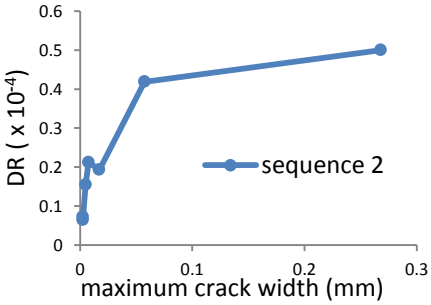

Figure 4.74: DR vs. crack max

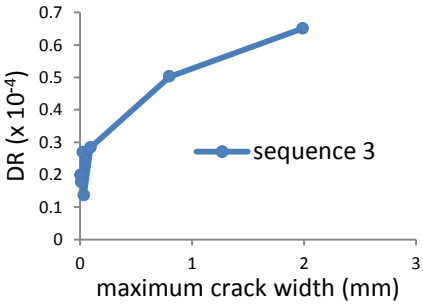

Figure 4.75: DR vs. crack max

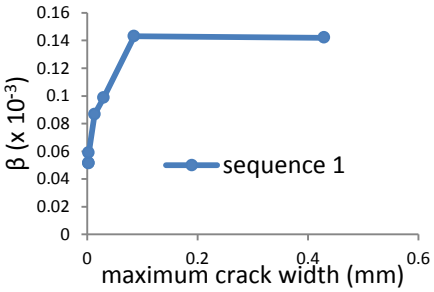

Figure 4.76: β vs. crack max

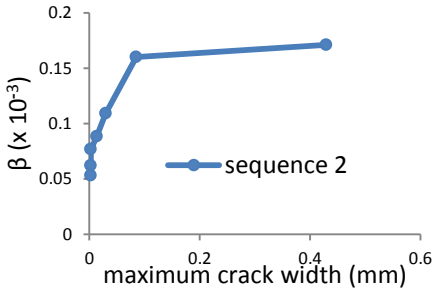

Figure 4.77: β vs. crack max

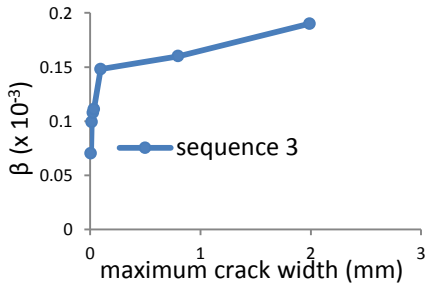

Figure 4.78: β vs. crack max

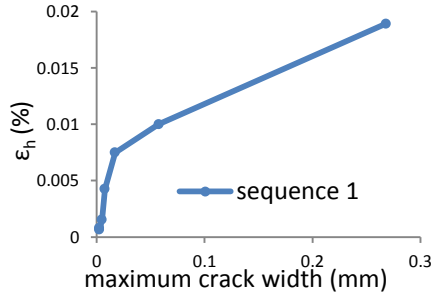

Figure 4.79: ε_h vs. crack max

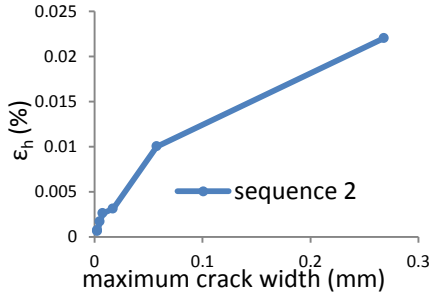

Figure 4.80: ε_h vs. crack max

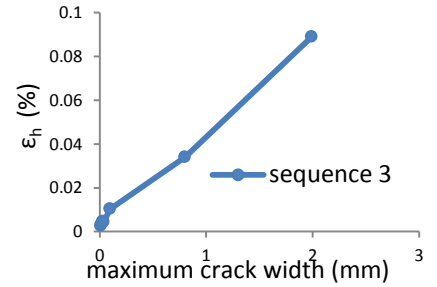

Figure 4.81: ε_h vs. crack max

Figure 4.82-4.93 shows evolution of damage and damage-indicator with excavation stages for wall, having door-opening at center, over 11-tunnel assembly; each data point corresponds to an

excavation stage, and shows value of damage-indicator at that particular excavation stage. Unlike the previous cases, tunnel-related damage started from the first excavation in this case. This is due to the fact that the excavation process started from the central portion for both excavation sequences, see Figure 106.

The last excavation stage inflicted much more damage than the other stages in excavation sequence 1, while the sixth excavation stage proved to be the one inducing most damage in excavation sequence 2. Overall, excavation sequence 2 inflicted much more damage than the excavation sequence 1.

The behaviour of wall is very different for the two excavation sequences. The only symptom showing a satisfactory correlation with damage for both sequences is $\Delta\theta$.

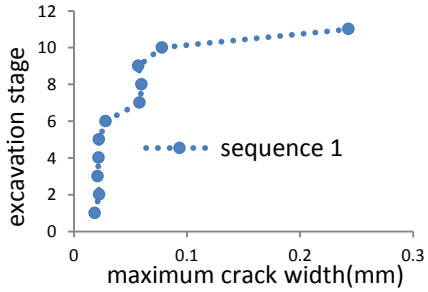

Figure 4.82: Crack max evolution

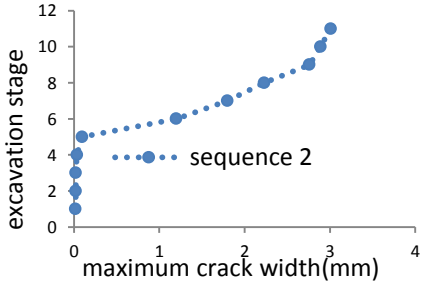

Figure 4.83: Crack max evolution

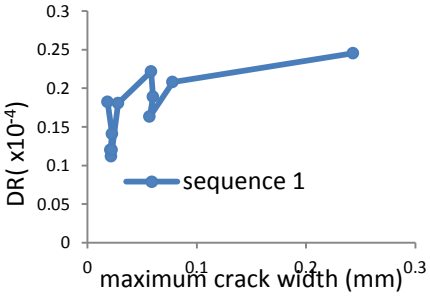

Figure 4.84: DR vs. crack max

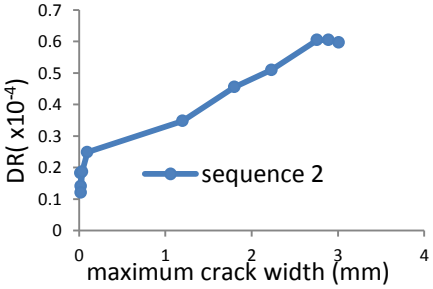

Figure 4.85: DR vs. crack max

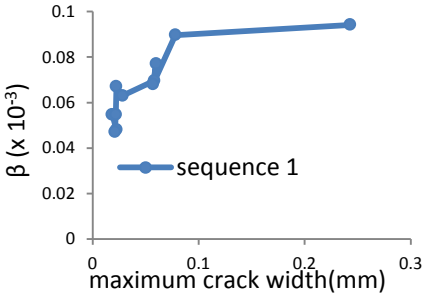

Figure 4.86: β vs. crack max

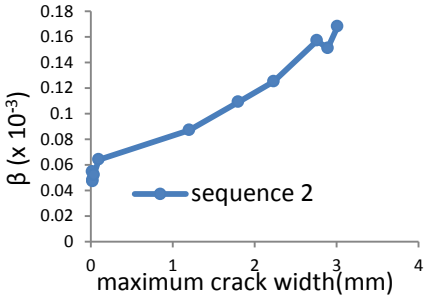

Figure 4.87: β vs. crack max

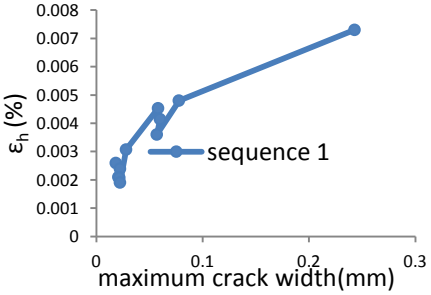

Figure 4.88: ε_h vs. crack max

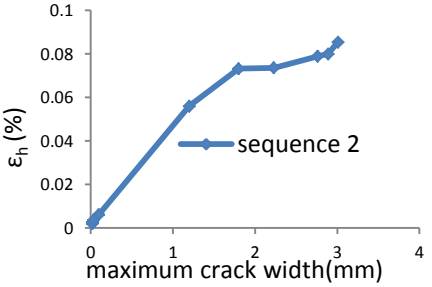

Figure 4.89: ε_h vs. crack max

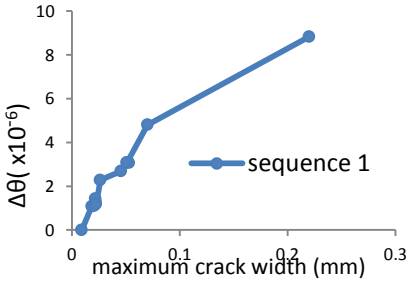

Figure 4.90: Δθ vs. crack max

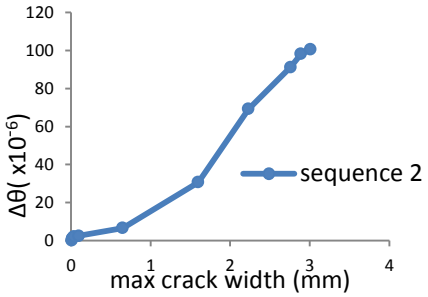

Figure 4.91: Δθ vs. crack max

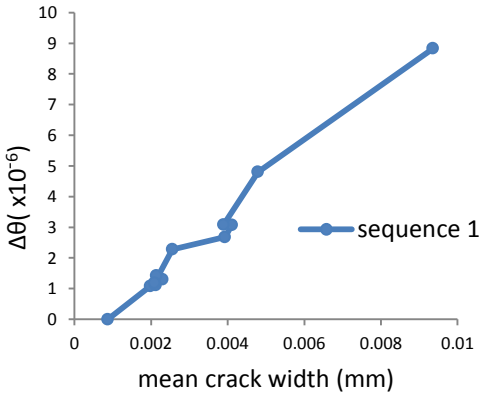

Figure 4.92: Δθ vs. crack mean

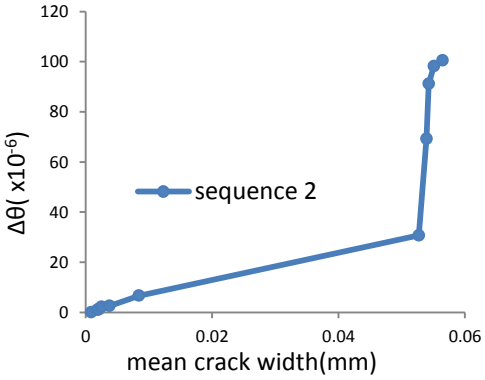

Figure 4.93: Δθ vs. crack mean

Figure 4.93-4.105 shows evolution of damage and damage symptoms with excavation stages for wall, having two door-openings away from center, over 11-tunnel assembly; each data point corresponds to an excavation stage, and shows value of damage symptom at that particular excavation stage.

The sequence 2 inflicted much more damage than the other two sequences. Excavation sequence 3 can be adopted for this case along with β as damage-indicator.

Excavation sequences 1 and 3 gave highly nonlinear and chaotic correlation between DR/ε_h and maximum crack width; excavation sequence 2 resulted in regular nonlinear relationship between DR and ε_h, and fairly linear relationship between average horizontal strain and maximum crack width. The correlation between β and maximum crack width is almost similar for all three sequences.

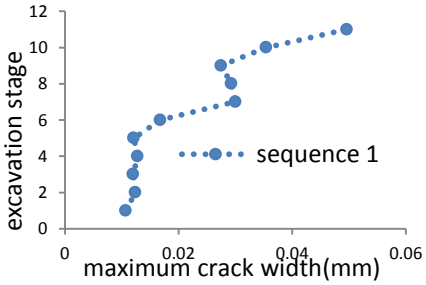

Figure 4.94: Crack max evolution

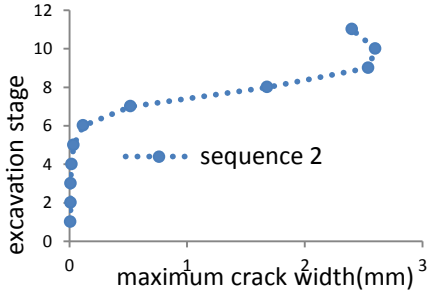

Figure 4.95: Crack max evolution

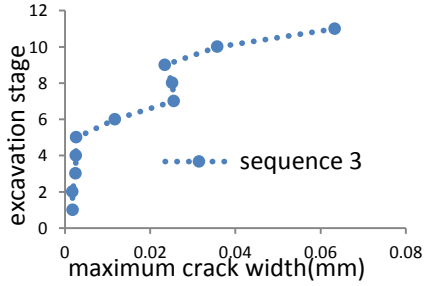

Figure 4.96: Crack max evolution

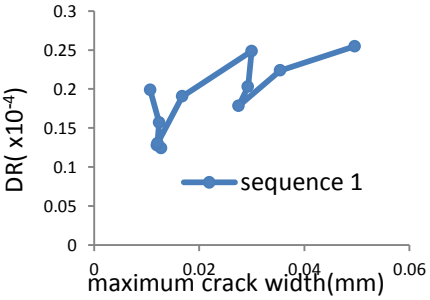

Figure 4.97: DR vs. crack max

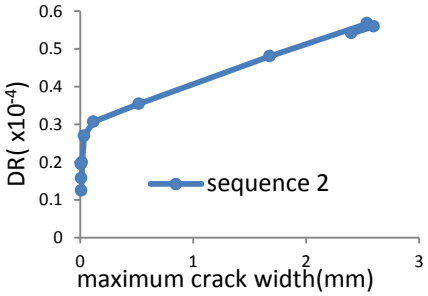

Figure 4.98: DR vs. crack max

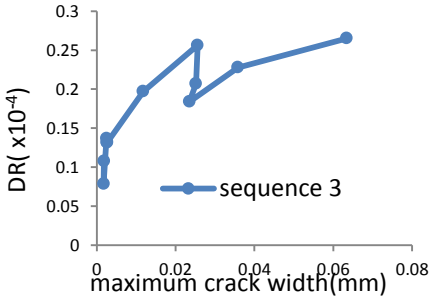

Figure 4.99: DR vs. crack max

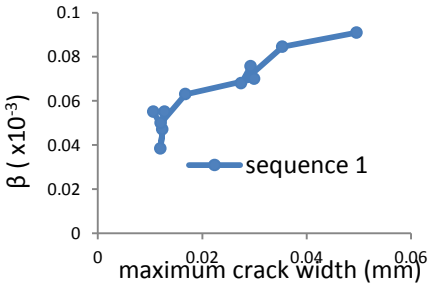

Figure 4.100: β vs. crack max

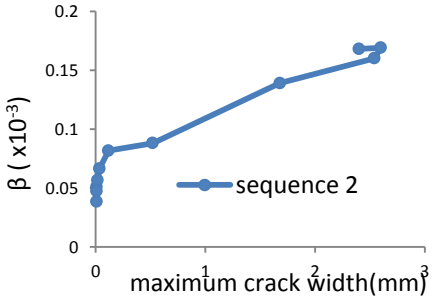

Figure 4.101: β vs. crack max

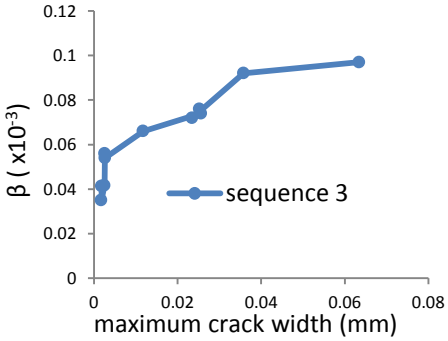

Figure 4.102: β vs. crack max

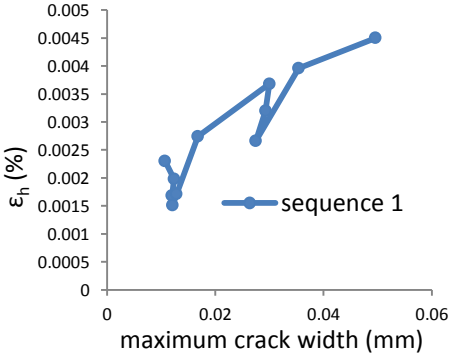

Figure 4.103: ε_h vs. crack max

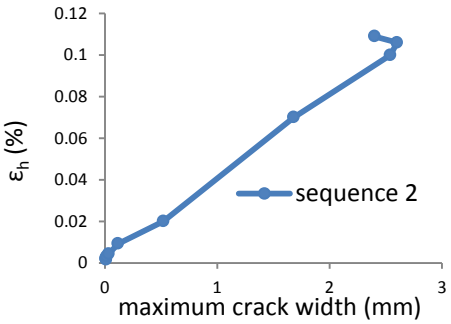

Figure 4.104: ε_h vs. crack max

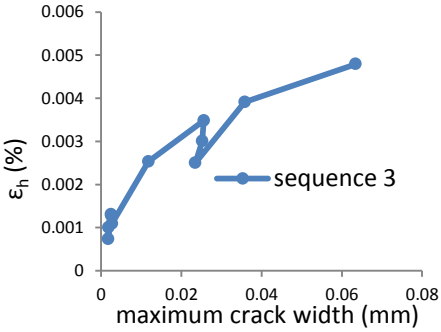

Figure 4.105: ε_h vs. crack max

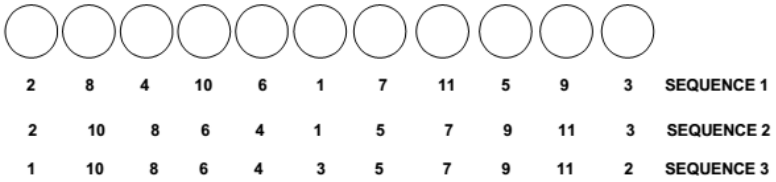

Figure 4.106: Sequences of excavation for the 11-tunnel assembly

Chapter 5

Conclusions and Recommendations

5.1. Conclusions

A coupled, 2D and nonlinear finite element analysis was conducted to study the effect of constructing closely-spaced microtunnels, in soils of varying stiffness', and under walls of various physical and mechanical characteristics. These closely-spaced microtunnels are required for an innovative base-isolation technique. The aim of this study was to investigate applicability potential of that innovative base-isolation technique; results were also presented for a study, conducted to identify possible damage symptoms.

Following conclusions can be drawn in the light of the study:

- The study demonstrates the applicability of innovative base-isolation technique for historic masonry construction without inflicting the damage that will impair functionality of building. The maximum values of various deformation indicators, encountered during study are: total settlement of about 40mm, tilt is about 0.2mm/m, angular distortion is about 0.0002, and maximum deflection ratio is about 0.00027.

- Sequence of tunnel construction has a significant effect on the damage sustained by masonry. Difference between correct and wrong choice, can be a difference between stable and unstable building. Study concluded that the sequence, in which the excavation starts from central region, will inflict much more damage than the one starting from ends.
- The type, and distribution of openings in wall, has a significant effect on damage susceptibility of masonry. The wall with only window openings is much less susceptible than the wall having openings for door and windows, and the wall having door opening in middle is most susceptible to damage than the other opening configurations.
- The wall, without any opening, is least susceptible to damage, relating to construction of innovative base-isolation technique. It will, at most, sustain hairline cracks for various conditions of soil and masonry, if its length is less than 20m.
- Nature of interface between soil and foundation of masonry is very crucial to damage susceptibility of masonry. The interface, providing resistance to relative tangential between soil and masonry, presents a favourable scenario. The interface, providing negligible resistance to relative tangential movements between soil and masonry, will lead to various levels of damage, depending on properties of materials, opening configuration of wall, length of wall, applied loads and excavation sequence.
- Weight of wall, or applied loads, has a significant effect on damage susceptibility of buildings. This study shows that the increase in stiffness of wall, due to increase in height, does not always counter the effect of increase in weight; It depends on presence of openings in wall, and its length to height ratio. In this study, damage susceptibility of walls with openings (coupled with smooth interface) increased with increase in weight, irrespective of length to height ratio. But the same was not the case with walls without openings. Taller walls, without openings, on 9 and 11-tunnel assembly, sustained less damage as compared to shorter walls, when subjected to tunnelling in same soil conditions, showing that increase in stiffness of wall due to increase in height overcame the effect of increase in weight. But opposite results were obtained for walls above 6 and 7-tunnel assembly. It should be also kept in mind that, in this study, volume loss was not kept constant; volume loss increased with increased in applied loads, and hence ground movements.
- Length of wall is very crucial to its damage susceptibility. Applicability potential of the proposed base isolation technique reduces with increase in length of wall. Tunnel construction should be carried along the longer side of building.
- It can be concluded from results that the applicability of the innovative base-isolation method also decreases with increase in height of building.
- Depth of tunnel construction will also influence the damage sustained by masonry, depending upon the length, height and weight of wall. It can be concluded that shallower depth should be preferred.

- It is of utmost importance to correctly access the stiffness of values of interface elements to be used in numerical model, as they have significant effect on the damage susceptibility of masonry wall.
- The result shows that the wall subjected to vertical ground movements, in transverse direction, due to closely-spaced microtunnels will not sustain a damage in hogging zone; it will either sustain significant damage in sagging area, or around openings, depending on nature of interface between soil and masonry.
- Different possible damage indicators have been monitored during simulations, some were taken from the literature and others newly proposed. In general no simple correlation can be identified between damage and any particular indicator. No indicator appears to neatly prevail over the others in all explored simulation cases. On average, the best damage indicators, capable of tracking damage evolution during construction, appear to be the maximum average horizontal strain, ε_h, and the maximum change in slope, $\Delta\theta$, which provide a nearly linear relationship with the maximum or the mean crack width in several cases. The worst damage indicators appear to be the tilt and the maximum differential settlement. These results suggest that "global" indicators based on the knowledge of few settlement values along the structure, which are typically monitored in common practice, are generally insufficient to reliably track the evolution of damage in a problem of closely-spaced multiple tunnels. "Local" indicators, unfortunately requiring a larger number of measurement points from closely-spaced sensors, appear much more representative of the actual damage extent in the present application.
- Masonry constructed with modern construction practices, adhering to the modern building codes, will sustain aesthetics-related damage in most conditions (read stiffness) of soil, provided soil has adequate strength.

5.2. Recommendations

Current work only dealt with transverse ground movements; the behavior of wall to longitudinal ground movements also needs to be investigated.

To realize the applicability of this technique on 2-5 story masonry buildings, built with modern construction practices, the effect of foundation also needs to be investigated.

REFERENCES

[1] P. Clemente, A. De Stefano and G. Barla, "Siesmic Isolation system for existing building". Italy Patent PCT/IB2011/000716, 2011.

[2] R. B. Peck, "Deep excavations and tunneling in soft ground," in *Proceeding 7th International conference on Soil Mechanics and Foundation Engineering*, 1969.

[3] D. N. Chapman, "Ground movements associated with trenchless pipelying operations," Loughborough University, 1992.

[4] M. Marshall, "Pipe-Jacked tunneling: Jacking loads and ground movements," 1998.

[5] E. Cording and W. H. Hansmire, "Displacements around ground tunnels," in *Fifth Pan-American conference on soil mechanics and foundation engineering*, Buenos Aires, 1975.

[6] G. W. Clough and B. Schmidt, "Design and performance of excavations and tunnels in soft ground," in *Soft Clay Engineering*, Amsterdam, Elsevier, 1981, pp. 569-638.

[7] M. P. O' Reilly and B. M. New, "Settlements above tunnels in United Kingdom: their magnitude and prediction," in *Tunneling*, London, 1982.

[8] W. J. Rankin, "Ground movements resulting from urban tunnelling: Predictions and effects," in *23rd annual conference of the engineering group of the Geological Society*, Nottingham,

1988.

[9] R. J. Mair and R. N. Taylor, "Bored tunnelling in urban environment," in *International conference on Soil Mechanics and Foundation Engineering*, Hamburg, 1997.

[10] T. I. Addenbrooke and D. M. Potts, "Twin tunnel interaction-surface and subsurface effects," *International Journal of Geomechanics*, vol. 1, pp. 249-271, 2001.

[11] D. N. Chapman, C. D. F. Rogers and D. V. L. Hunt, " Investigating the settlement above closely spaced multiple tunnel constructions in soft ground," in *World Tunnel congress*, Amsterdam, 2003.

[12] S. Divall, R. J. Goodey and R. N. Taylor, "Ground movements generated by sequential Twin tunnelling in over-consolidated clay," in *2nd conference on physical modelling in Geotechniques*, Deflt, 2012.

[13] D. V. L. Hunt, "Predicting the ground movements above twin tunnels constructed in London Clay," University of Birmingham, 2005.

[14] J. B. Burland and C. P. Wroth, "Settlement of buildings and associated damage," in *Settlement of stuctures*, Cambridge, 1974.

[15] M. Boscardian and E. J. Cording, "Building response to excavation-induced settlement," *ASCE-Journal of Geotechnical Engineering*, vol. 115, no. 1, pp. 1-21, 1989.

[16] S. Timoshenko, Strength of Materials part 1:Elementary theory and problems, Newyork: D. Van Nostrand, 1955.

[17] J. Burland, B. Broms and . V. De Mello, "Behaviour of foundations and structures," in *SOA report, session 2, Proc. 9th Conf. SMFE*, Tokyo, 1977.

[18] B. Schmidt, "Settlements and ground movements associated with tunneling in soil," University of Illinois, 1969.

[19] C. Sagaseta, "Analysis of undrained soil deformation due to ground deformation," *Géotechnique*, vol. 37, pp. 301-320, 1987.

[20] R. J. Mair, R. N. Taylor and J. B. Burland, "Prediction of ground movements and assessment of risk of building damage due to bored tunnelling," in *International Symposium on Geotechnical Aspects of Underground Construction in Soft ground*, Rotterdam, 1996.

[21] J. B. Burland, "Assessment of risk of damage to buildings due to tunneling and excavations," in *Invited Lecture, International Conference on Eathquake Geotechnical Engineering*, Tokyo, 1995.

[22] J. N. Franzius, D. M. Potts and J. B. Burland, "The response of surface structures to tunnel construction," *Proceedings of the ICE - Geotechnical Engineering*, vol. 159, no. 1, pp. 3-17, January 2006.

[23] H. Netzel and F. J. Kaalberg, "Numerical Damage Risk Assessment Studies on adjacent buildings in Amsterdam," in *Internation conference of Geotechnical and Geological Engineering*, Melbourne, 2000.

[24] H. D. Netzel, "Building response due to ground movements," IOS press, March, 2009.

[25] D. M. Potts and T. I. Addenbrooke, "A structure's influence on Tunneling-Induced ground movements," *ICE-Journal of Geotechnical Engineering*, vol. 125, no. 2, pp. 109-125, 1997.

[26] B. A. Zeeshan, A. D. Stefano and S. Invernizzi, "Effects of using innovative Seismic Isolation technique on masonry: tunnelling work required," in *Earthquake Resistant Engineering Structures IX*, A Coruna, 2013.

[27] S. J. Boone, "Assessing construction and settlement-induced building damage: a return to fundamental principles," in *Underground construction, Institution of Mining and Metalurgy*, London, 2001.

[28] DIANA Finite Element Analysis, User's Manual, Release 9.4.4, TNO Building Construction

& Reseacrch, 2012.

[29] P. B. Lourenco, "Computational strategies for Masonry Structures," Delft, Netherlands, 1996.

[30] J. G. Rots, "Computational modelling of concrete fracture," Delft, Netherlands., 1988.

[31] J. A. Charles and H. D. Skinner, "Settlement and tilt of low rise buildings," *Proceedings of Institute of civil engineers, Geotechnical Engineering,* vol. 157, pp. 65-75, 2004.

[32] G. Giardina, A. V. V. d. Graaf, M. A. N. Hendriks, J. G. Rots and A. Marini, "Numerical analysis of a masonry façade subject to tunnelling-induced settlements," *Engineering Structures,* vol. 54, pp. 234-247, march 2013.

[33] B. u. A. Zeeshan, A. De Stefano, E. Matta and A. Quattrone, "Monitoring of existing Masonry buildings during construction of an innovative Base-isolation system," in *6th International Conference on Structural Health Monitoring of Intelligent Infrastructure, 9-11 December, SHMII-6,* Hongkong, 2013.

[34] J. G. Rots, P. Nauta, G. M. A. Kusters and J. Blaauwendraad, "Smeared crack approach & fracture localization in concrete," *Heron,* vol. 30, no. 1, p. 48, 1985.